Development and validation of a novel UPLC-ELSD method for the assessment of lipid composition of nanomedicine formulation

Mathieu Varache, Mathieu Ciancone, Anne-Claude Couffin

Development and validation of a novel UPLC-ELSD method for the assessment of lipid composition of nanomedicine formulation.

Mathieu Varache[1,2*], Mathieu Ciancone[1,2], Anne-Claude Couffin[1,2]

[1]*CEA-LETI, Microtechnologies for Healthcare and Biology Division, 17 rue des Martyrs, 38054 Grenoble Cedex 09, France*

[2]*Université Grenoble Alpes, 38000 Grenoble, France*

[*]Corresponding author: VaracheM@cardiff.ac.uk

Abstract

Lipid nanocarriers incorporating glycerides, polyethylene glycol (PEG)-stearates and phospholipids have attracted great attention for *in vivo* diagnostic, *in vivo* imaging, activated or non-activated targeted drug delivery. For quality control purposes, the development of appropriate methods for the quantification of their lipid components is needed. In the present study, we developed an analytical method for lipid quantification in formulated nanoparticles. PEG-stearates and glycerides were analyzed in a single run by RP-UPLC-ELSD using a two-step gradient elution program, while the analysis of phospholipids was accomplished by HILIC-UPLC-ELSD after isolation using an SPE silica column. Using both isolated compounds and commercial lipid standards, calibration curves were produced using second-order polynomials to attain the quantitative evaluation of each lipid excipient. Relative standard deviation of all analytes was between 0.9% and 5.3% for intra-day precision and recovery ranged from 83.5% to 112.2%. The presented method was successfully implemented to study the manufacturing process and stability of the formulated lipid excipients during long-term storage and accelerated conditions. The formulation lipid yield was determined and found equal to 82.5%.

Keywords: lipid nanoparticles, UPLC, ELSD, reversed-phase HPLC, HILIC, SPE, triglycerides, phospholipids, polyethylene glycol, validation

1. Introduction

Since the early stages of nanotechnologies, nanomedicines (NMs) have received great attention due to their ability to overcome the limitations of traditional drug delivery modalities. Although numerous nanosized carriers have led to tremendous research activities and demonstrated significant therapeutic advantages for a multitude of biomedical applications, to date, only 50 NMs have been marketed [1]. In comparison to conventional formulation technology, their clinical translation is far more complex and requires an expensive and time-consuming process for which many issues have been identified as obstacles [2–4]. For instance, an adequate understanding of how they interact with biological systems is fundamental, which requires comprehensive physicochemical characterization. In addition, the use of proper, rational and specific characterization methods is essential for large-scale production, according to Good Manufacturing Practices (GMP) standards, and quality controls are needed to achieve batch-to-batch consistency on a daily basis. The latter requirement is particularly important since batch-to-batch variation of NMs affects their physicochemical properties, pharmacokinetic parameters, and/or pharmacodynamics interactions [2,3].

Despite the arsenal of NMs currently under preclinical development or in clinical trials, lipid nanocarriers, especially liposomes, are dominant on the NMs market and were the first-FDA approved NMs [5,6]. In addition to natural and/or synthetic phospholipids as their main constituent, liposomes often contain functionalized lipids, such as PEGylated materials containing polyethylene glycol (PEG) chains that are intended to support escape from the reticuloendothelial system [7]. As an alternative to liposome-based drug carriers, solid lipid nanoparticles (SLN) have been developed in order to increase loading capacity of lipophilic drugs and overcome chemical/physical stability issues [8–10]. General ingredients include solid lipid(s), such as triglycerides, partial glycerides, fatty acids, steroids and waxes.

For more than 10 years, our research group has been developing lipid nanocarriers known as Lipidots®, which have demonstrated utility in the delivery of therapeutic agents, and for disease monitoring and diagnosis by fluorescence imaging [11,12]. As a nanocarrier, Lipidots® have been proved to possess a high colloidal stability over several months. In addition, particle size and viscosity of the core can be tuned, resulting in high payloads, controlled drug release and improved drug bioavailability to appropriate biological sites [13]. More recently, our lipid nanocarriers showed great potential as innovative delivery systems of protein antigens by chemical modification of the shell [14,15]. Far more complex than liposomes, our lipid nanocarriers are composed of a lipid core comprising a mixture of saturated and unsaturated glycerides, and a surfactant shell comprising a mixture of PEGylated surfactants and phospholipids. To facilitate potential clinical utility and regulatory approval, a large panel of

analytical and physicochemical methods have been developed and used to extensively characterize our Lipidots® platform [16,17]. Subsequently, we sought to develop and validate an analytical method that would allow the quantification of all individual excipients belonging to lipid-based nanoparticles.

From an analytical point of view, the quality of these pharmaceuticals must be assured through the development of appropriate methods to characterize and quantify their lipid components and degradation products [18,19]. For this purpose, high-performance liquid chromatography (HPLC) is the technique of choice because of its ability to separate lipids into different classes or species based on their alkyl chain lengths and/or head group polarity [20–23]. For instance, reversed-phase (RP)-HPLC has become the most popular method for separating and analyzing triglyceride species in oils and fats, because it operates on the principle of both chain length and degree of unsaturation of fatty acids, thus enabling separation of individual triglyceride molecules [24,25]. Concerning the analytical measurements of PEGylated materials, methods involving coordination complexes, enzymatic/antibody detection or chromatographic techniques have been developed [26,27]. The analysis of phospholipids has also been accomplished by RP-HPLC, normal phase (NP)-HPLC or hydrophilic interaction liquid chromatography (HILIC) [28–31].

Over the past 10 years, ultra-performance liquid chromatography (UPLC) has greatly improved resolution over traditional HPLC analysis in a wide range of applications. UPLC uses sub-2 µm porous stationary phase particles and operates with high linear velocities >9000 psi. The significant advantages of UPLC over HPLC include dramatic increases in resolution, speed and sensitivity, which simplify the characterization of complex samples like those containing lipids [32–36].

Evaporating light-scattering detection (ELSD), first described by Charlesworth [37], is a quasi-universal detector than can detect any analyte less volatile than the mobile phase [38,39]. ELSD has become popular to detect and monitor the separation of poor UV-absorbers, such as phospholipids [40–44], PEG [45–48] and triglycerides [49–52]. This detection technique was chosen in these studies for several reasons. First, this equipment is well established in the quality control of liposome suspensions [53,54]. Second, contrary to UV and refractive index (RI) detection, solvent selection and gradient elution are not limiting factors [55,56]. Finally, compared with charged aerosol detectors (CAD), ELSD has a very low background noise with solvents commonly used in RP-HPLC lipid analysis (methanol, isopropanol, acetonitrile) [57].

In this work, two distinct chromatographic methods were used: a RP-UPLC-ELSD method for the determination of PEGylated surfactants and glycerides, a HILIC-UPLC-ELSD method for

the assessment of phospholipids. The full analytical method was applied to study the manufacturing process and stability of the formulated lipid excipients during long-term storage and under accelerated conditions.

2. Materials and Methods

2.1 Materials

Suppocire NC™ (SC) was purchased from Gattefossé (Saint-Priest, France). Myrj™ S40, polyethylene glycol (PEG) 40 stearate (S40), and Super Refined Soybean oil (SB) were obtained from Croda Uniquema (Chocques, France). Lipoid S75 (S75, soybean lecithin) was provided from Lipoid GmbH (Ludwigshafen, Germany). All these excipients were pharmaceutical grade and used as received for preparing lipid nanoparticles. L-α-phosphatidylcholine (Soy PC, >99% purity, 840054C) and L-α-phosphatidylethanolamine (Soy PE, >99% purity, 840024C) used as standards at respectively 25 mg/mL and 10 mg/mL in chloroform were purchased from Avanti Polar Lipids, Inc. (Alabaster, USA). For Soy PC, the unsaturated fatty acids are palmitic (C16:0, 14.9%) and stearic (C18:0, 3.7%) and the unsaturated fatty acids are oleic (C18:1, 11.4%), linoleic (C18:2, 63%) and linolenic (C18:3, 5.7%). For Soy PE, the unsaturated fatty acids are palmitic (C16:0, 17.7%) and stearic (C18:0, 2.2%) and the unsaturated fatty acids are oleic (C18:1, 5.0%), linoleic (C18:2, 65.5%) and linolenic (C18:3, 7.4%). Acetonitrile (ACN), methanol (MeOH), isopropanol (IPA), hexane (HEX), diethyl ether (DEE) and chloroform ($CHCl_3$), ammonium formate, ammonium acetate, sodium acetate and formic acid (50% in water) were supplied by Sigma Aldrich (Saint-Quentin-Fallavier, France). Standards of triacylglycerols (TAGs) including trilinolein (LLL) and triolein (OOO) were obtained from Nu-check (Elysian, USA). All chemicals and reagents were analytical grade and were used without any further purification. HPLC-grade water (MQ, specific resistance=18.2 MΩ.cm) was obtained from a Classic DI MK2 water purification system (Elga, UK) and was used in all experiments. Lipid nanoparticles were formulated using a VCX750 Ultrasonic processor from Sonics (Newtown, USA) equipped with a 3 mm-diameter microtip. The balance was an XP105 from Mettler Toledo (Columbus, USA), the centrifuge was a Heraeus Pico 17 from Thermo Scientific (Waltham, USA) and the vortex was a Reax top from Heidolph (Swabach). The measurement of pH in chromatographic mobile phases was determined using a FiveEasy Bench Meter from Mettler Toledo (Columbus, USA) calibrated using commercial buffers before each measurement.

2.2 Chromatographic conditions for lipid quantification using UPLC-ELSD analysis

Chromatographic analysis of the lipid nanoparticles components was performed using an Acquity UPLC H-Class system from Waters (Milford, USA) coupled with an Alltech 3300

Evaporating Light Scattering detector (ELSD) from Grace (Columbia, USA). Separation of the different compounds was achieved using two chromatographic methods involving two different columns, both equipped with a guard column of the same material (1.6 µm, 5 x 2.1 mm, 90 Å, Waters). On the one hand, quantification of SC, SB and S40 was performed using reversed-phase mode with a CORTECS UPLC C18 column (1.6 µm, 150 x 2.1 mm, 90 Å, Waters). For the following, this method will be referred to as QMC18**.** Separation was achieved using a gradient program involving 3 eluents: water (eluent A), methanol (eluent B) and 25% v/v ACN in IPA (eluent C). For better reproducibility, the latter mobile phase was gravimetrically prepared daily. Chromatographic separation was carried out according to the following scheme: t_0 min: 30%A/70%B at 0.25 mL/min, $t_{3.0}$ min: 10%A/90%B at 0.3 mL/min, $t_{7.0}$ min: 100%B at 0.3 mL/min, $t_{22.0}$ min: 35%B/65%C at 0.3 mL/min, $t_{25.0}$ min: 35%B/65%C at 0.3 mL/min, $t_{25.1}$ min: 30%B/70%C at 0.25 mL/min and finally isocratic conditions (30%A/70%B) for 4.9 min at 0.25 mL/min. The total duration of the method was 30 min. The drift tube temperature of the detector was maintained at 45°C with the optimum flow rate of the nebulizing gas (nitrogen) fixed at 2.0 L/min. The gain was fixed at 4. On the other hand, phospholipids belonging to S75 were quantified by hydrophilic interaction liquid chromatography (HILIC) using a CORTECS UPLC HILIC column (1.6 µm, 150 x 2.1 mm, 90 Å, Waters). Hereafter, this method will be referred to as QMHILIC**.** Separation was achieved using a gradient program with two eluents. 10 mM ammonium formate (pH=3) was mixed with ACN in a ratio 5:95 (v/v) to produce mobile phase A or 50:50 (v/v) to produce mobile phase B. Chromatographic separation was carried out using the following scheme: t_0 min: 100%A, $t_{5.0}$ min: 65%A/35%B, $t_{8.0}$ min: 65%A/35%B, $t_{9.0}$ min: 100%A and finally isocratic conditions (100%A) for 8 min. The flow rate of the eluent was 0.5 mL/min. The drift tube of the detector was maintained at 60°C with a flow of N_2 fixed at 2.5 L/min and the gain was set at 2. In both chromatographic methods, the injection volume was 5 µL, the column and autosampler temperatures were fixed at 40°C and 25°C, respectively. Data acquisition and processing were performed using Empower 3 chromatographic software through Waters SAT/IN module.

2.3 Chromatographic conditions for lipid identification using UPLC-TOF/MS analysis

An Agilent-1260 UPLC system coupled to a 6230B TOF mass spectrometer (Agilent Technologies, Santa Clara, USA) was used. For the separation, a CORTECS UPLC C18 column (1.6 µm, 150 x 2.1 mm, 90 Å, Waters) equipped with a guard column (1.6 µm, 5 x 2.1 mm, 90 Å, Waters) was used. The working parameters were established as follows: flow rate 0.3 mL/min, column temperature 45 °C, injection volume 5 µL, and auto-sampler ambient temperature (20-25°C). Separation was achieved using a gradient program with 2 eluents: methanol (eluent A) and 25% v/v ACN in IPA (eluent B). Both mobile phases contained

ammonium acetate (0.05% w/v) and sodium acetate (0.001% w/v). Chromatographic separation was carried out using the following scheme: t_0 min: 100%A, $t_{15.0}$ min: 35%A/65%B, $t_{18.0}$ min: 35%A/35%B, $t_{19.0}$ min: 100% and finally isocratic conditions (100%A) for 11 min. The optimized mass spectrometric conditions are positive electrospray ionization (ESI) mode, drying gas (N_2) flow rate 8.0 L/min, drying gas temperature 325°C, nebulizer pressure 50 psi, fragmentor potential 175 V, capillary voltage 3500 V, octapole radio frequency voltage (Oct RFV) 750 V and skimmer voltage 65 V. Data acquisition and analysis were performed using MassHunter software (Agilent Technologies). A calibrating solution (G1969-85000, ES-TOF Tuning Mix) was used daily to obtain accurate mass measurements for each peak from the total ion chromatogram. The ESI-MS spectra were obtained at m/z range of 100 to 1500. Samples (SB and SC) were dissolved at 85 and 95 µg/mL, respectively, in a mixture of IPA and MeOH (1:1, v/v).

2.4 Isolation of Myrj™ S40 components using preparative HPLC

Isolation was carried out using a Waters Auto Purification LC/MS system, equipped with a 2545 Binary Gradient Module, a 515 HPLC pump, a 2767 Sample Manager, a 2998 Photodiode Array (PDA) detector and a 3100 mass detector. Separation was achieved using an XBridge BEH Prep C18 column (5 µm, 19 x 100 mm, 130 Å, Waters) equipped with a guard column (5 µm, 19 x 10 mm, 130 Å, Waters). The flow rate was 14.0 mL/min, and the injection volume was 300 µL. The separations were carried out at room temperature (20-25°C) and used a gradient program with two eluents: water (eluent A) and methanol (eluent B). The chromatographic separation was carried out according to the following scheme: t_0 min: 80%A/20%B, $t_{3.0}$ min: 15%A/85%B, $t_{15.0}$ min: 13%A/87%B, $t_{18.0}$ min: 100%B, $t_{35.0}$ min: 100%B, $t_{36.0}$ min: 80%A/20%B, $t_{40.0}$ min: 80%A/20%B. Prior to the isolation, Myrj™ S40 was dissolved at 250 mg/mL in a mixture of $CHCl_3$ and MeOH (2:1, v/v). Detection was performed in positive ionization electrospray mode with the following source conditions: capillary voltage 3.5 kV, cone voltage 35 V, source temperature 150°C, desolvation temperature 450°C, desolvation gas flow 900 L/h, and cone gas flow 50 L/h. Instrument control and data acquisition were performed using MassLynx SCN627 4.1 software. Fraction collection was triggered automatically by signals from the MS detector at m/z = 1538, 1732, 1760, 1584, 1952 and 1980. The minimum intensity threshold was fixed at 200,000. For each collected fraction, methanol was evaporated by rotary evaporation (50°C) and the fractions were freeze-dried and stored at -20°C. The purification yield was around 45%.

2.5 Solid phase extraction of the phospholipids

PC and PE phospholipids from S75 excipient were quantified after separation using a normal solid phase extraction (SPE) method [58]. SEP-PAK Silica Vac cartridges (3 cc, 200 mg, 55-105 µm) were used, together with an extraction manifold from Waters (Milford, USA). After

conditioning with 3 mL hexane, 500 µL of a solution containing 25 mg/mL total excipient materials was loaded and slowly eluted by gravity to ensure good retention of phospholipids. Non-polar lipids were eluted with 2 mL of a mixture of HEX:DEE (8:2, v/v) followed by 2 mL of HEX:DEE (1:1, v/v). Phospholipids were then recovered in 5 mL volumetric flasks by elution with 2 mL of methanol followed by 2.5 mL of a mixture of $CHCl_3$:MeOH:MQ (3:5:2, v/v/v). Volumetric flasks were filled up to the mark with methanol, leading to a solution containing 2.5 mg/mL of total lipids. Cleaning efficacy was determined by measuring the concentration of each excipient with or without SPE using QMC18. Recovery was evaluated by comparing two calibrations curves performed for Soy PC and Soy PE, with or without SPE, *i.e.* performed with or without adding the other excipients (SC, SB and S40).

2.6 Validation

2.6.1 Calibration

Individual stock solutions of SB (10 mg/mL), SC (20 mg/mL), PEGylated components (PEG-OH, PEG-C16 and PEG-C18, 5 mg/mL each), Soy PC (2.5 mg/mL) and Soy PE (1 mg/mL) were prepared in a mixture of $CHCl_3$:MeOH (2:1, v/v). Using the same solvent mixture, SB, SC and PEGylated components (PEG-OH, PEG-C16 and PEG-C18) stock solutions were diluted to achieve standard concentrations in the range of 136 to 408 µg/mL, 46-136 µg/mL and 62-186 µg/mL, respectively. A calibration curve for PEG-OH was also performed in the range of 2 to 6 µg/mL. For Soy PC and Soy PE, calibrations were performed with or without the other excipients (SB, SC and PEGylated components spiked at their theoretical concentrations), meaning with or without applying the SPE protocol. With SPE, Soy PC and Soy PE solutions were prepared in the range from 606 to 1820 µg/mL and 83 to 250 µg/mL, respectively. Volumetric flasks were then made up to the mark using a mixture of $CHCl_3$ and MeOH (2:1, v/v) and the SPE protocol was applied. Final concentrations of Soy PC and Soy PE were in the range of 61 to 182 µg/mL for PC and 9-26 µg/mL for PE. Without SPE, Soy PC and Soy PE stock solutions were directly diluted with $CHCl_3$:MeOH:MQ (3:5:2, v/v/v), without the other excipients, to achieve standard concentrations in the range of 61 to 182 µg/mL for Soy PC and 9-26 µg/mL for Soy PE. Each solution was prepared and systematically injected in triplicate using the suitable analytical method described above (QMC18 and QMHILIC). For the quantification of PC and PE, we used the calibration curves obtained after the SPE process.

2.6.2 Detection and quantification limits

The limit of detection was determined for PEG-OH and Soy PE using calibration curves at low concentrations where linear models can be applied. Calibration curves were obtained in the range from 2 to 6 µg/mL for PEG-OH and 9-26 µg/mL for Soy PE. The limits of detection (LOD) and quantification (LOQ) were thus estimated based on the standard deviations of the y-intercepts of regressions analysis (σ) and the slope (S), by the following equations LOD = 3.3

σ/S and LOQ = 10 σ/S. Since the calibration curve for SB, SC and PC could not be fitted using linear models, the LOD values were calculated by injecting samples containing known low concentrations of analytes and blank solutions. LOD and LOQ were then calculated by the following equations LOQ = $3.h_{max}.R$ and LOQ = $10.h_{max}.R$ where R is the response factor (concentration divided by the peak height corresponding to the low concentration sample) and h_{max} is the height obtained for blank solutions between RT ± 10 FWHM (RT = retention time of the compound and FWHM = full-width-half-maximum). Low concentrations were 42, 79 and 5 µg/mL respectively for SB, SC and Soy PC. For SB and SC, the highest peaks were used (RT at 19.4 and 17.5 min, respectively).

2.6.3 Accuracy and precision using lipid standards

The accuracy and precision were measured by analyzing lipid standards solution using 3 concentrations (60%, 100% and 120% of target concentration). Stock solutions of lipid standards were mixed together in a mixture of $CHCl_3$ and MeOH (2:1, v/v) to attain 15, 25 and 30 mg/mL of total lipids. These solutions were prepared singly. The analysis of SB, SC and S40 were performed after diluting each solution of total lipids equivalent to 0.6, 1.0 and 1.2 mg/mL. For the QMC18 method, 3 diluted solutions per concentration were prepared. For the QMHILIC method, the SPE protocol was performed in triplicate. All samples were injected in triplicate. Concentrations of each component were then calculated for each injection using the calibration curves previously obtained. The accuracy was reported as a relative error of the measured concentration over the nominal concentration (RE, %), and the precision was expressed as the relative standard deviation (RSD, %).

2.6.4 Precision using nanoparticle suspensions

The intra-day (repeatability) and inter-day (intermediate precision) of the analytical method were evaluated over a period of 3 days using a single nanoparticle suspension (100 mg/mL). Each day, 3 pre-weighed tubes containing 1 mL of suspension were frozen then freeze-dried. After 24 h, each tube was weighed, and the obtained mass compared to the theoretical mass to evaluate the precision on the freeze-drying step and express the concentration of each component per mL. For each tube, the overall process of preparation and quantification described above (section sample preparation) was performed. All samples were injected in triplicate. The system repeatability was also evaluated by injecting a single sample 6 times using QMC18 and QMHILIC methods. Concentration of each component was then obtained for each injection using the calibration curves obtained previously. Precision was expressed as the relative standard deviation (RSD, %). The percent recovery (%) was calculated by using the theoretical and experimental concentrations of the lipids.

2.7 Manufacturing of lipid nanoparticle suspensions

Lipid nanoparticles (LNP) were prepared according to our previously reported method [13,59,60]. In a typical procedure leading to 50 nm diameter particle dispersion (F50), an oil premix was prepared including, respectively, 85, 255, and 65 mg of SB, SC, and S75. After homogenization of the lipid phase at 40°C, the continuous phase, composed of 345 mg of Myrj^{TM} S40 dissolved in 1X PBS aqueous buffer (1X Phosphate Buffer Saline: 10 mM phosphate, 154 mM NaCl, pH 7.4) was introduced. The vial was then placed in a 20°C water bath and sonication cycles were performed during 20 min with intervals of 10 s “Pulse On” and 30 s “Pulse Off”. After filtering the suspension of nanoparticles (at a lipid equivalent of 200 mg/mL) through a 5 µm cellulose Millipore membrane, the purification step was carried out overnight using dialysis (1X PBS, MWCO: 12 kDa). Lipid nanoparticles were finally formulated at a theoretical total concentration of lipids of 100 mg/mL and then filtered through a 0.22 µm cellulose Millipore membrane for sterilization before immediate characterization.

2.8 Analytical sample preparation from nanoparticle suspensions

For each suspension of 50 nm nanoparticles prepared at 100 mg/mL of total lipids, 1 mL was transferred to an Eppendorf tube and freeze-dried overnight, using a Freezone 2.5 Liter Benchtop freeze dry system from Labconco (Kansas City, USA). In a typical procedure, solutions at 25 mg/mL were prepared by dissolving 50 mg of lyophilized powder in a mixture of $CHCl_3$:MeOH (2:1, v/v) in a 2 mL volumetric flask and left to stand for 1 h to allow precipitation of salts. For the quantification of SC, SB and S40, 200 µL of previous solutions were diluted in 5 mL volumetric flasks using a mixture of $CHCl_3$ and MeOH (2:1, v/v) to obtain solutions at 1 mg/mL of total lipids. Each dilution was performed in triplicate. Samples were analyzed in triplicate by using QMC18 method. S75 phospholipids were quantified after extraction using normal SPE as described in section 2.5, where 500 µL of the solution at 25 mg/mL of lyophilized materials was loaded onto the cartridges. Samples were then submitted to QMHILIC method and analyzed in triplicate. For clarity, concentration of the lipid components along the analytical procedure is presented in Table S1.

2.9 Functional aspect of the analytical method

2.9.1 Following-up of the manufacturing process

For a suspension containing 50 nm lipid nanoparticles, the lipid excipients were quantified at 5 steps of the manufacturing process: before sonication (reference), after sonication, after filtration on a 5 µm cellulose Millipore membrane, after dialysis and after filtration on 0.22 µm cellulose Millipore membrane. This final suspension corresponds to a standard suspension of nanoparticles theoretically at 100 mg/mL of lipids. To avoid a lack of reproducibility due to the premix preparation, lipid and continuous phases were originated from the same parent

solution. At each step of the protocol, one of the samples was freeze-dried. Then, for each sample, the entire dried powder was dissolved in $CHCl_3$:MeOH (2:1, v/v), left to stand for 1 h and diluted to 25 mg/mL (theoretical concentration). The analytical procedure previously described was then applied on each solution. Results are expressed as the percentage of components compared to quantities measured before sonication.

2.9.2 Stability of excipients in nanoparticles under storage and accelerated thermal conditions

Stability of the excipients have been evaluated under storage conditions at 4°C for 50 nm (F50), 80 nm (F80) and 120 nm (F120) formulations using our analytical procedure. The corresponding composition of the formulations is presented in Table S2. At t = 0, 15, 30, and 60 days, 1 mL of each suspension (a single suspension per size) was taken and freeze-dried before applying our overall process of quantification. To study degradation of excipients under accelerated thermal conditions, freshly prepared suspensions of F50, F80 and F120 were stirred at 300 rpm in an incubator at 60°C. At t = 3, 7, 15 and 30 days, 1 mL of each suspension was collected and immediately freeze-dried before applying our overall quantification process. Each sample was injected in triplicate using QMC18 and QMHILIC methods. Results are presented as residual quantities of each compound compared to their respective quantities at t = 0. The amount of the excipients for the suspensions of F80 and F120 nanoparticles are different to that of F50 (Table S2). In order to use the same calibration, our sample preparation protocol was adapted (in terms of sample weight and dilution) to inject the amount of excipients (target concentration) previously defined for 50 nm lipid nanoparticles.

3. Results & Discussion

The aim of this study was to develop an analytical method to quantify each component of our lipid nanoparticle (LNP) formulation. Such a method may facilitate the bench-to-bedside translation of our nanomedicine by ensuring reliability and reproducibility during large-scale manufacturing. The excipients of the nanoparticle matrix consist of a lipid core containing a mixture of lipids and surfactants, Super Refined™ Soybean oil (SB) oil and Suppocire NB™ (SC), stabilized by a shell of Lipoid® S75 (S75) and Myrj™ S40 (S40). The nanoparticles were manufactured by dispersion via ultrasonication of the lipid phase containing SB, SC and S75 excipients in an aqueous phase (PBS only) containing PEGylated surfactants (S40). Fig. 1(a) illustrates the whole core/shell architecture of the nanoparticles whilst detailing the chemical structures of the lipid excipients.

3.1 Composition of lipid excipients

All crude excipients used for LNP manufacturing were carefully selected for their GMP grade and provided from manufacturers guaranteeing long-term supply in large amount, thus

ensuring future large-scale production. Each of them was used as received and stored as recommended by manufacturers. None of the raw materials consisted of one pure lipid but were instead composed of a mixture of parent components. As certificates of analysis (CoA) mention only the percentages of different fatty acid chains, fine identification of the glyceride-based compounds had to be performed using different separative techniques coupled with mass spectrometry (MS) to elucidate the composition of different mono- (MAGs), di- (DAGs) and triglycerides (TAGs) within each crude excipient. Isolation of lipid compounds is also crucial to be able to produce standards when none are commercially available, which can be used to produce calibration curves for quantitative analysis.

Myrj™S40 (S40). Based on supplier information, S40 is a non-ionic surfactant described as a PEG fatty acid ester (PEGylated stearate) with an ethylene oxide (EO) distribution of around 40 units. According to the CoA, the fatty acid esters are a mixture of palmitate and stearate saturated fatty acids, usually termed C16:0 and C18:0, respectively. Using LC/MS analysis performed on a preparative scale (Fig. S1), 3 peaks were observed at 7.2, 14.5 and 19.1 min and respectively assigned to polyethylene glycol (PEG-OH), polyethylene glycol palmitate (PEG-C16) and polyethylene glycol stearate (PEG-C18), respectively, with distribution of EO between 25 and 47 units. Indeed, single charged sodium adducts $[M+Na]^+$ showed mass differences of 238 (acid palmitic minus OH) and 266 (acid stearic minus OH) respectively for PEG-C16 and PEG-C18, compared to PEG-OH. As an example, for a species corresponding to 32 units of EO (exact mass = 1426.85), single charged sodium adducts $[M+Na]^+$ were observed at m/z = 1449.99, 1688.27 and 1716.27 for PEG-OH, PEG-C16 and PEG-C18, respectively. Finally, preparative reversed-phase HPLC was performed to collect each PEGylated species, thus allowing quantitative analysis through calibration curves.

Super Refined™ Soybean oil (SB). SB is a complex mixture of acylglycerols with saturated and unsaturated fatty acids, 73-93% being unsaturated fatty acids (FA) (Fig. 1(b)). The saturated fatty acids are palmitic (C16:0) and stearic (C18:0) and the unsaturated fatty acids are oleic (C18:1), linoleic (C18:2) and linolenic (C18:3) acid. Due to the low polarity of these compounds (log P>5), the use of water for their analysis by RP-HPLC is generally avoided in the mobile phase, leading to non-aqueous reversed-phase (NARP) chromatography. The most commonly used solvents for NARP chromatography of oils are low polarity solvents such as acetonitrile/dichloromethane, isopropanol/acetonitrile, isopropanol/acetonitrile/hexane with or without gradient elution [25,61–64]. Here, SB was analyzed by NARP-UPLC coupled with a time-of-flight (TOF) mass spectrometer (MS) by using a linear gradient of methanol/isopropanol/acetonitrile (Fig. S2(a)). As the intensity of the total ion current is relatively low using non-aqueous solvent system, ammonium acetate and sodium acetate were added to the solvent in order to increase the ionization efficiency without affecting the retention time [65]. Under these conditions, molecular adducts of sodium $[M+Na]^+$ and ammonium

$[M+NH_4]^+$ were formed, as observed in the MS spectra obtained for standards of trilinolein (LLL) and triolein (OOO) (Fig. S2(b) and Fig. S2(c), respectively). For LLL, $[M+Na]^+$ and $[M+NH_4]^+$ adducts were observed at m/z = 901.72 and 896.76, respectively, which is in good agreement with the theoretical values (m/z = 901.73 and 896.77, respectively). For OOO, $[M+Na]^+$ and $[M+NH_4]^+$ adducts were observed at m/z = 907.77 and 902.81, respectively, which is also in very good agreement with the theoretical vales (m/z = 907.77 and 902.82, respectively). In order to identify the peaks obtained for SB (Fig. S2(a)), experimental molecular masses (sodium and ammonium adducts) obtained for each peak were collected and assigned to TAG species (Table S3) with reference to the literature [36,49,66,67]. On reversed-phase columns, it is very well known that the separation of TAGs occurs according to the combined effect of chain length of the FA-moieties contained in a given TAG species plus their degree of unsaturation; each double bond reduces the retention by the equivalent of about 2 carbon atoms. The analysis of TAG mixtures is often complicated by the occurrence of nearly identical molecular species or critical pairs, which exhibit similar chromatographic behavior on reversed-phase columns. Critical pairs are described as molecular species with the same equivalent carbon number (ECN) defined by the following equation: ECN = CN – (2 x NDB), where CN is the sum of carbon atoms in the aliphatic residues and NDB is the sum of double bonds per TAG [68]. Here, thanks to the assignment of each peak, the elution of TAGs belonging to SB occurred according to the ECN and each peak is actually a cluster of TAGs possessing the same ECN (Fig. S2(a) and Table S3).

Suppocire NB™ (SC). According to the manufacturer, SC is a mixture of mono- (MAGs), di- (DAGs) and triglycerides (TAGs) with saturated fatty acids and an overall hydroxyl value of 20-30% (Fig. 1(b)). The saturated fatty acids are mostly lauric (C12:0), myristic (C14:0), palmitic (C16:0) and stearic (C18:0). In a similar way to SB, SC was analyzed by using NARP-UPLC-TOF/MS (Fig. S3). Each peak was assigned using $[M+Na]^+$ and $[M+NH_4]^+$ adducts and the ECN was calculated for each acylglycerol (Table S4). Having a very similar chemical composition as SB, the elution of acylglycerol species belonging to SC occurred with increasing ECN. As SC is only composed of saturated fatty acids, each peak corresponds to one acylglycerol species, contrary to SB, for which each peak is a cluster of TAGs with the same ECN. While it was possible to precisely identify TAGs from SB, we were not able to identify precisely the composition of each peak (fatty acids composition) as MS spectra showed only the presence of intense protonated molecular $[M+Na]^+$ and $[M+NH_4]^+$ adduct ions, and not their respective mono- and diacyglycerol ions. For instance, it is impossible to distinguish tripalmitin (PPP, TAG(C16:0/C16:0/C16:0)) from palmitoyl-myristoyl-stearoyl-glycerol (PMS, TAG(C14:0/C16:0/C18:0)). However, this analysis was able to determine the ECN of each peak. Surprisingly, we found that SC was only composed of DAGs and TAGs.

Lipoid® S75 (S75). Phospholipids (PLs) are amphiphilic and polar molecules with a structure similar to triacylglycerols, except that a phosphate group is typically found in the *sn*-3 position of the glycerol backbone. As a mixture of PLs, S75 is composed of 71.6% phosphatidylcholine (PC) blended with less than 9.9% phosphatidylethanolamine (PE) and 1.8% lysophosphatidylcholine (LPC). According to the manufacturer, their saturated fatty acids are mostly palmitic (C16:0, 17-20%) and stearic (C18:0, 2-5%) and their unsaturated fatty acids are oleic (C18:1, 8-12%), linoleic (C18:2, 58-65%) and linolenic (C18:3, 4-6%). Contrary to the PEGylated species belonging to S40, preparative HPLC on S75 was not needed because standards of PLs possessing a very similar composition of fatty acids (see materials section) were commercially available. These standards (L-α-phosphatidylcholine (soy PC) and L-α-phosphatidylethanolamine (soy PE)) were purchased from Avanti Polar Lipids, Inc (Alabster, USA) [69] for direct identification based on the retention time and for quantitative analysis through calibration curves.

3.2 Method development

During the development process, the challenge was to set-up a reliable, simple and sensitive method leading to a precise quantification of each excipient (SB, SC) or the major species of each excipient (i.e. PEG-OH/PEG-C16/PEG-C18 for S40, PC/PE for S75). One particular obstacle to be overcome was to properly separate and sensitively detect PC and PE from S75, while avoiding interferences due to the presence of the other crude excipients. By using only one mode of chromatography (reversed-phase) and a single run, this appeared challenging and consequently, two distinct chromatographic methods were needed for analyzing lipids from SB, SC and S40 crude excipients on the one hand, and phospholipids (PC/PE) from S75 on the other.

3.2.1 RP-UPLC-ELSD analysis of SB, SC and S40 excipients

Herein, a novel reversed-phase UPLC-ELSD method was successfully developed for the separation and detection of the lipids belonging to SB, SC and S40 crude excipients. This method, named QMC18 in the manuscript, involved a two-step gradient elution program (Table 1). The first step (from 0 to 7.0 min) corresponds to the separation of PEGylated surfactants belonging to S40 crude excipient using a linear gradient elution with a water/methanol mobile phase. This method, originally developed on a HPLC system by Lee *et al.* [70], was transferred and optimized to our UPLC system. Using this linear gradient program, PEGylated surfactants of S40 (PEG-OH, PEG-C16 and PEG-C18) were baseline separated in the order of increasing time of 1.7, 6.3 and 6.9 min (Fig. 2(c)). As previously described, highly purified standards of PEG-OH, PEG-C16 and PEG-C18 were obtained by preparative HPLC (Fig. S4). Calibration curves of S40 (184-552 µg/mL) and PEG-OH, PEG-C16, and PEG-C18 standards (62-186 µg/mL) were used to determine the proportion of each PEGylated surfactant

within the S40 crude excipient. The identified PEG components were calculated to represent 71.3% (w/w) of S40 crude excipient composed of PEG-OH (30.1% (w/w), PEG-C16 (34.6% (w/w) and PEG-C18 (35.3% (w/w)). The second step of the reversed-phase UPLC-ELSD method (from 7.0 to 25.0 min) corresponds to the separation and detection of acylglycerol species belonging to SB and SC excipients employing the same linear gradient of methanol/isopropanol/acetonitrile that was previously used for their analysis by NARP-UPLC-TOF/MS. This method allowed the elution to be achieved without using dichloromethane or hexane solvents, which are often incompatible with the PEEK-based tubing and rings of conventional HPLC systems. As shown in Fig. S5 and S6, the chromatograms of SB and SC obtained by ELSD mirrored those acquired using TOF/MS. A correlation was thus been made regarding the elution of acylglycerols that still occurred in the order of increasing ECN. As this quantification method had to be as fast and simple as possible, it was not necessary to separate critical pairs, which would have led to increased complexity of the final signature of the excipients.

3.2.2 HILIC-UPLC-ELSD analysis of S75 excipients

The analysis of S75 crude excipients using the QMC18 method did not produce well-defined peaks that could be separated from the other lipid excipients (data not shown). Indeed, RP-HPLC enables the separation of lipid species as a function of their lipophilic tails and PL classes are often difficult to separate, especially when they contain more than one sub-component [28,31,71]. Moreover, separation of the individual components within the different PL classes was not required so we aimed to develop a method that would provide only an effective baseline separation of the different phospholipid classes (PE, PC). HILIC, first suggested by Alpert [72], has become a good alternative to RPLC for separating polar compounds, such as phospholipids, because it is particularly effective at class separation [73,74]. HILIC combines the features of both NPLC and RPLC, as it employs polar stationary phases, such as silica, which are typical of NPLC, with an organic-dominant mobile phase, such as solvent mixtures containing > 50-70% ACN in water or volatile buffers, which is typical of RPLC [75]. The pure theoretical HILIC retention mechanism is mainly partitioning of polar compounds between the organic-rich mobile phase and the water-enriched layer that is partially immobilized on the stationary phase, however, it may also involve more than a simple liquid/liquid partitioning [76]. Separation of different phospholipid classes is generally achieved by NPLC, whereby distinctive retention occurs according to their polar head group (PE, PC, etc.) [41]. However, NPLC uses mobile phases consisting of unpolar solvents (like hexane, isooctane or chloroform) as the main constituents, which are not so convenient to handle due to their chemical compatibility, volatility and toxicity. Moreover, it is highly time-consuming to switch a chromatographic system from RPLC to NPLC, whereas shifting from RPLC to HILIC

is straightforward. Therefore, we developed an HILIC-UPLC-ELSD method (QMHILIC) allowing an effective baseline separation of S75 phospholipids classes (PE and PC). Identification of S75 phospholipids was achieved by comparison of the retention times with those of the reference materials (Soy PE and Soy PC), as outlined in Fig. 3(a) and Fig. 3(b). PE and PC were well separated under gradient conditions in the order of increasing time of 4.2 and 5.9 min, eluting according to decreasing polarity PE > PC [43]. By using appropriate calibration curves performed with S75 crude excipients and reference materials (Soy PE and Soy PC), S75 was found to be composed in weight of PC (75.0%) and PE (12.2%), which is in good agreement with the proportions provided by the manufacturer (71.6 and 9.9% for PC and PE, respectively).

3.2.3 Sample preparation

Sample preparation is one of the most critical issues in analytical method development. For the development and validation of our analytical method, 50 nm formulations (F50) were exclusively used. Batches of nanoparticles were manufactured by ultrasonication, leading to a final theoretical concentration of lipids of 100 mg/mL. The concentrations of SB, SC, S75 and S40 were theoretically equal to 11.33 mg/mL, 34.00 mg/mL, 8.67 mg/mL and 46.00 mg/mL, respectively (Table S1). According to the previously evaluated crude excipients' composition, the concentration of PEG components was 32.79 mg/mL, which is equivalent to 9.88, 11.34 and 11.57 mg/mL of PEG-OH, PEG-C16 and PEG-C18, respectively (Table S1). The concentration of PC and PE were 6.07 mg/mL and 0.87 mg/mL, respectively (Table S1). Thus, the theoretical total quantifiable concentration of lipids was 84.56 mg/mL. As quantification of excipients relies on detection of the individual species, disintegration of the nanoparticles must be performed first. Methods involving hydro-organic solvents are traditionally used for the quantification of encapsulated entities such as drugs and dyes, however the solvents are known to destabilize the interface of droplets, which induces solubilization of the active ingredients and precipitates the excipients [17,77]. Thus, a transparent solution of all the excipients was required for lipid quantification. Here, a freeze-drying step was selected to destabilize the oil/water emulsion, and allow the collection of the dried excipients (Fig. 4). After weighing the lyophilized powder, lipid excipients were dissolved in a mixture of $CHCl_3$:MeOH (2:1, v/v) providing a transparent and homogeneous solution at a theoretical lipid concentration of 25 mg/mL. Thereafter, two distinct sample preparation processes were used to quantify the corresponding lipids using QMC18 or QMHILIC (Fig. 4). Concentrations of each component along the sample preparation process are summarized in Table S1. For the analysis of SB, SC and PEG components, the initial solution was diluted 25-fold in $CHCl_3$:MeOH (2:1, v/v) to reach a final theoretical lipid concentration of 1 mg/mL. For the analysis of S75 crude excipients using QMHILIC, the challenge arose from the presence of interference peaks, which was even more

problematic because of the low abundance of PLs within the formulation compared to the other lipids. As outlined in the HILIC-UPLC-ELSD chromatogram of the whole lipid formulation (diluted 10-fold compared to the extracted sample), a huge amount of non-polar lipids (DAGs and TAGs from SB and SC) eluted at the beginning of the gradient run (Fig. S7). More importantly, a broad peak corresponding to PEGylated surfactants occurred between 4-8 min and interfered with those of PE and PC (eluting at 4.2 and 5.9 min, respectively). Therefore, a silica SPE protocol originally developed for the extraction of PLs from milk [58] was applied in order to isolate S75 crude excipients and remove the interference peaks from the other lipids. This isolation method effectively removed 100% (w/w) of SB and SC, and 75% (w/w) of S40 (PEG-C16 and PEG-C18) (Fig. S7 and Table S5). An acceptable recovery of PLs was also achieved. From 40 to 120% of the analysis/target concentrations, recoveries of PC and PE varied from 107.3-99.1 and 101.6-118.4%, respectively (Table S6). Calculations of the recoveries were made using the equations of two calibration curves for PC and two others for PE, performed with or without SPE, respectively, *i.e.* with or without the other excipients (S40, SB and SC). Comparison of the results obtained in both cases showed that remaining PEGylated surfactants (around 25%) tend to overestimate the amount of PC and PE, especially at low concentrations. Elution of S75 crude excipients during SPE indicated a 10-fold dilution of the initial solution, leading to PC and PE contents of 151.6 and 21.7 µg/mL, respectively.

3.2.4 Chromatographic signatures of the reverse-engineered nanoformulation

Beside obtaining a whole lipid signature of the nanoformulation, chromatographic peaks were specifically assigned by considering peak overlap that occurs due to the complexity and molecular similarity of the lipid species. As outlined by blue arrows in Fig. S8, overlap between peaks of SB and SC occurred. According to the identification by TOF/MS (NARP-UPLC-TOF/MS method), peak overlap mostly appeared for TAGs possessing the same ECN number (ECN = 46, 48 and 50), except the one at 17.4 min occurring between LLnL (ECN = 40) from SB and a TAG from SC (ECN = 42), which could be assigned to trimyristin (MMM) if composed of the same fatty acids (TAG(C14:0/C14:0/C14:0)). A typical QMC18 chromatogram of a nanoparticle suspension is presented in Fig. 2(d). The peaks were symmetrical, well resolved, well detected, mostly baseline separated, and have reproducible retention times compared to those of crude excipients. Peaks corresponding to SC and S40 also overlapped at retention times of 9.9, 10.9 and 12.1 min were not assigned for the quantification. For SB and SC, it was assumed that the selected peaks mirrored the content of the entire raw materials, contrary to S40. Indeed, the peak at 1.7 min corresponding to PEG-OH has almost disappeared in the chromatogram obtained for the nanoparticle suspension, emphasizing the necessity of quantifying each PEG component rather than the total lipid content of the raw material. For

QMHILIC, peaks corresponding to PE and PC at retention times of 4.2 and 5.9 min, respectively, were identified in the chromatogram corresponding to the nanoparticle suspension and were used for the quantification (Fig. 3(c)). Further investigations also demonstrated that the selected peaks used for the quantification were reliable markers of the lipid composition. Overall, our chromatographic methods allowed the analysis of a complex mixture of excipients belonging to lipid nanoparticles. While rarely used for lipids in drug delivery systems, the concept of lipid profiling or lipid fingerprinting could be used for quality authentication of lipid nanoparticles in the context of quality control testing of pharmaceuticals. More importantly, these analytical methods ideally suit the requirements of the pharmaceutical industry for performing quality control of excipients as raw materials. To provide more clarity, the analytical parameters of QMC18 and QMHILIC were summarized in Table 2.

3.3 Method Validation

The aim of this study was to investigate the validation of the developed analytical procedure to prove its applicability for intended quantification of lipid excipients, prior to industrial transfer. Methods were validated with respect to linearity, limits of detection (LOD) and quantification (LOQ), precision and accuracy (recovery rate) using lipid standards. In addition, repeatability and intermediate precision were evaluated on the quantification of lipid excipients from a nanoparticle suspension. As outlined in Table 3, target concentrations have been defined according to the composition of each lipid excipient and the sample preparation. To facilitate method validation, target concentrations of PEG-OH, PEG-C16 and PEG-C18 were considered equal to 100, 115 and 115 µg/mL, respectively.

3.3.1 Calibration

Consistent with previous reports, ELSD responses in the defined ranges showed a non-linear relationship (Fig. S9) due to the dependence of the efficiency of prevalent light-scattering processes, namely Rayleigh scattering, Mie scattering, and reflection-refraction, on the average particle size [37,78,79]. As previously reported for the analysis of lipids using ELSD, a second-order polynomial (quadratic) of the following form was used as a fitting model: $Y = a_0X^2 + a_1X + a_2$, where X represents the concentration in µg/mL, a_0, a_1, and a_2 are constants and Y is the peak area [21,38,80–82]. This model produced R^2 (coefficient of determination) values > 0.9977 indicating that the fitting was statistically valid (Table 3). Quadratic calibration plots might be too laborious to use in routine quality control studies, due to consequent standards preparation and data processing. An alternative approach would involve logarithmic linearization by plotting log(peak area) versus log(lipid concentration) [78]. Applied to our results, linear functions with good correlation coefficients were obtained for each

lipid (Table S7). While this mathematical transformation is acceptable for ICH [83], it can lead to an experimental error distortion by simple data flattening [84].

3.3.2 Detection and quantification limits

Assessment of LOD and LOQ values were more complex than usual since the calibration curves were fitted using quadratic equations. In our study, two methodologies were used, depending on the lipid and its range of concentration. For PEG-OH, given its low concentration in our samples, calibration between 2.0 and 6.0 µg/mL was performed and a good linearity between peak area and concentration was obtained (R^2 = 0.9835). However, the use of a quadratic equation was deemed more appropriate ($1611.8x^2 + 4182.9x + 6342$, R^2 = 0.9962). For PE, an acceptable linear relationship was observed between 8.7 and 26.0 µg/mL (R^2 = 0.9932) but the quadratic fitting was still more appropriate (R^2 = 0.9977). These linear fittings were used to determine LOD and LOQ values from the SD of the response and the slope. In these studies, calibration curves for SB, SC and PC leading to a linear relationship between peak areas versus concentration were not performed. Consequently, the LOD and LOQ values were calculated by comparing the measured signals from samples having known low concentrations of the analyte with blank solutions. The results are presented in Table 3. The LODs of PE and PEG-OH were 2.9 and 0.8 µg/mL, respectively. These findings are in good agreement with previous reports performed under similar experimental conditions (3.4 µg/mL (PE) and 1 µg/mL (PEG) reported by Donato [43] and Zabaleta [46], respectively).

3.3.3 Repeatability and accuracy using lipid standards

Repeatability (RSD) and accuracy (RE) were determined by analyzing three replicates at three different concentrations (60, 100 and 120% of the target concentration). Each replicate was injected in triplicate. For intra-day precision (repeatability), triplicate measurements of three standard solutions (60, 100 and 120%) on the same day were recorded. Accuracies of both methods were determined by calculating the percent recoveries of the analytes in the spiked samples, based on their theoretical concentration. As presented in Table 4, the repeatability of all analytes ranged from 0.9% to 5.3% and the accuracy from 83.5% to 112.2%. For lipid analysis repeatability, a value lower than 5% is generally accepted [22,41,54,85].

3.3.4 Repeatability and intermediate precision on nanoparticle suspensions

To make sure that this analytical method could be applied for daily quality control along a manufacturing process, when consistent precisions is required, intra- and inter-day precisions were evaluated directly on a single nanoparticle suspension. The results obtained in these studies are presented in Table 5. A specific calibration was performed for PEG-OH at low concentration (range: 2.0-6.0 µg/mL, equation: $Y = 1611.8x^2 + 4182.9x + 6342$, R^2 = 0.9962) due to its removal during dialysis. Relative standard deviations for system repeatability were ≤

2.6%, except for PEG-OH (5.9%) as the concentration was close to LOQ. The intra-day precision (repeatability) of all analytes was ≤ 7.1% (RSD) and inter-day precision (intermediate precision) ranged from 3.9% to 6.3% (excluding PEG-OH). Overall recovery ranged from 84.4% to 97.3% (excluding PEG-OH). Using the overall concentrations (n=9), total lipid content was assessed and the manufacturing yield (theoretical vs experimental concentrations) was determined to be 82.5%. For lipid analysis, repeatability < 5% and intermediate precision < 10% are generally expected [22,41,54,85]. As part of the quantification process, repeatability and intermediate precision of the freeze-dried process were 0.37% and 0.52%, respectively.

3.4 Functional aspect of analytical methods

3.4.1 Following-up of manufacturing process

The use of analytical methods as quality control tools to enable monitoring of nanoparticle preparation was one of our main goals. Using our validated analytical methods, the lipid components of 50 nm lipid nanoparticles were quantified after each step of the nanoparticle preparation process and used to calculate the percentage of each component compared to their initial quantities measured before sonication (Fig. 5 and Table S8). After sonication, the amount of all lipids, apart from PE, remained stable, demonstrating that most lipids are not degradaded during sonication. After filtration through a 5-µm filter, around 25% of lipids were lost, presumably due to elimination of non-formulated lipids that could be visually observed on vial walls. While the content of most lipids was not affected by dialysis (~ 6-12% loss), PEG-OH was completely eliminated during this step, presumably due to its high water-solubility. Indeed, PEG-OH does not display fatty acid chains, which limits its role as a surfactant in the O/W nanoemulsion and promotes its escape from the nanoparticle shell. PE was also removed by dialysis (12% loss), albeit to a lesser extent, probably due to the increased water solubility conferred by its free amine. Unsurprisingly, the final step (sterilization by filtration 0.22-µm) did not affect the amount of lipids.

3.4.2 Stability of lipid excipients during long-term storage and accelerated thermal conditions of suspensions

Previous studies have demonstrated that our lipid nanoparticles are highly stable (colloidal stability) at 4°C for more than 18 months [13]. Storing the nanoparticles at 4°C prevents degradation of encapsulated thermal-sensitive drugs/dyes and efficiently prevents Ostwald ripening. Herein, the above-developed analytical method was used to evaluate the stability of the lipid excipients (once formulated) under recommended cold stored conditions (4°C for 2 months) and under accelerated thermal conditions (60°C for 1 month). Excipient recovery (% lipid content at t = 0 h) from 50 nm lipid nanoparticles is presented in Fig. 6. Under cold storage conditions, the proportion of each lipid remained constant over 60 days, while under

accelerated conditions, a significant time-dependent decrease in lipid recovery was observed for PE, PC and SB. Similar results were observed for 80 nm (F80) and 120 nm (F120) nanoparticles (Fig. S10). Degradation thus occurred only on phospholipids and unsaturated TAGs (SB). In a similar timeframe, colloidal stability was rapidly lost under accelerated thermal conditions (results not shown). As previously reported for liposomes, the hydrolysis of phospholipids by hydrolytic cleavage of the ester functionalities in presence of water generates lysophospholipids and free fatty acids that prevent them from acting as surfactants and strongly affects the physical stability of the O/W nanoemulsion by promoting fusion of the nanoparticles, mainly by Ostwald ripening [20,21,86]. Hydrolysis of PE, PC and SB was assessed by plotting lipid excipient concentration against storage time on a semi-logarithmic scale. As previously observed for phosphatidylcholine, it followed pseudo-first order kinetics [87,88]. For F80, first-order constants of 2.49 x 10^{-3}, 1.42 x 10^{-3} and 2.09 x 10^{-3} h^{-1} were calculated for PE, PC and SB, respectively, suggesting that the degradation rate of PE is slightly faster than that of SB and PC. A similar trend was found for F50 and F120. Although a quantitative decrease of peak areas for PE and PC was observed during degradation, no peak corresponding to lysophospholipids was detected and only free fatty acids were observed at the column void volume (Fig. S11). Similarly, no additional peak was observed for SB (Fig. S12).

4. Conclusion

In this study, we have developed and validated a set of analytical methods for the quantification and identification of PEGylated surfactants, glycerides and phospholipids in lipid-based nanoformulations, thereby enabling the contents of individual lipid excipients to be monitored during nanoparticle formulation. The ability of this analytical method to study the degradation of lipids within these nanoformulations provided additional qualitative information in addition to the colloidal features of the nanoparticles. With minor modifications, this method may be applied to other similar lipids and employed in quality control of commercial manufacture of lipid-based nanomedicines. The reproducibility and accuracy of this method highlights its potential utility in quality control processes and represents an important step towards the implementation of “stability tests” required by regulatory agencies, which includes the development of suitable methods for the detection and quantification of degradation products.

Acknowledgement

This work was financially supported by BpiFrance and is part of the NICE project aiming to foster the clinical and industrial development of nanomedicine products. The authors greatly acknowledge Dr. Elaine Ferguson for her comments and suggestions during the preparation

of this manuscript. The authors also would like to thank Dr. Thibault Gutel for providing the UPLC-TOF/MS equipment.

Conflicts of interest

The authors declare no conflict of interest.

References

[1] J.-B. Coty, C. Vauthier, Characterization of nanomedicines: A reflection on a field under construction needed for clinical translation success, J. Controlled Release. (2018). doi:10.1016/j.jconrel.2018.02.013.

[2] M.K. Teli, S. Mutalik, G.K. Rajanikant, Nanotechnology and nanomedicine: going small means aiming big, Curr. Pharm. Des. 16 (2010) 1882–1892.

[3] S. Tinkle, S.E. McNeil, S. Mühlebach, R. Bawa, G. Borchard, Y.C. Barenholz, L. Tamarkin, N. Desai, Nanomedicines: addressing the scientific and regulatory gap, Ann. N. Y. Acad. Sci. 1313 (2014) 35–56. doi:10.1111/nyas.12403.

[4] V. Sainz, J. Conniot, A.I. Matos, C. Peres, E. Zupanǒiǒ, L. Moura, L.C. Silva, H.F. Florindo, R.S. Gaspar, Regulatory aspects on nanomedicines, Biochem. Biophys. Res. Commun. 468 (2015) 504–510. doi:10.1016/j.bbrc.2015.08.023.

[5] J. Shi, P.W. Kantoff, R. Wooster, O.C. Farokhzad, Cancer nanomedicine: progress, challenges and opportunities, Nat. Rev. Cancer. 17 (2017) 20–37. doi:10.1038/nrc.2016.108.

[6] J.M. Caster, A.N. Patel, T. Zhang, A. Wang, Investigational nanomedicines in 2016: a review of nanotherapeutics currently undergoing clinical trials, Wiley Interdiscip. Rev. Nanomed. Nanobiotechnol. 9 (2017) e1416. doi:10.1002/wnan.1416.

[7] M.L. Immordino, F. Dosio, L. Cattel, Stealth liposomes: Review of the basic science, rationale, and clinical applications, existing and potential, Int. J. Nanomedicine. 1 (2006) 297–315.

[8] R.H. Müller, R. Shegokar, C.M. Keck, 20 years of lipid nanoparticles (SLN and NLC): present state of development and industrial applications, Curr. Drug Discov. Technol. 8 (2011) 207–227.

[9] W. Mehnert, Solid lipid nanoparticles Production, characterization and applications, Adv. Drug Deliv. Rev. 47 (2001) 165–196. doi:10.1016/S0169-409X(01)00105-3.

[10] R.H. Müller, M. Radtke, S.A. Wissing, Nanostructured lipid matrices for improved microencapsulation of drugs, Int. J. Pharm. 242 (2002) 121–128. doi:10.1016/S0378-5173(02)00180-1.

[11] J. Mérian, R. Boisgard, P.-A. Bayle, M. Bardet, B. Tavitian, I. Texier, Comparative biodistribution in mice of cyanine dyes loaded in lipid nanoparticles, Eur. J. Pharm. Biopharm. Off. J. Arbeitsgemeinschaft Für Pharm. Verfahrenstechnik EV. 93 (2015) 1–10. doi:10.1016/j.ejpb.2015.03.019.

[12] L. De Matteis, D. Jary, A. Lucía, S. García-Embid, I. Serrano-Sevilla, D. Pérez, J.A. Ainsa, F.P. Navarro, J. M. de la Fuente, New active formulations against M. tuberculosis: Bedaquiline encapsulation in lipid nanoparticles and chitosan nanocapsules, Chem. Eng. J. 340 (2018) 181–191. doi:10.1016/j.cej.2017.12.110.

[13] T. Delmas, A.-C. Couffin, P.A. Bayle, F. de Crécy, E. Neumann, F. Vinet, M. Bardet, J. Bibette, I. Texier, Preparation and characterization of highly stable lipid nanoparticles with amorphous core of tuneable viscosity, J. Colloid Interface Sci. 360 (2011) 471–481. doi:10.1016/j.jcis.2011.04.080.

[14] T. Courant, E. Bayon, H.L. Reynaud-Dougier, C. Villiers, M. Menneteau, P.N. Marche, F.P. Navarro, Tailoring nanostructured lipid carriers for the delivery of protein antigens:

Physicochemical properties versus immunogenicity studies, Biomaterials. 136 (2017) 29–42. doi:10.1016/j.biomaterials.2017.05.001.

[15] E. Bayon, J. Morlieras, N. Dereuddre-Bosquet, A. Gonon, L. Gosse, T. Courant, R.L. Grand, P.N. Marche, F.P. Navarro, Overcoming immunogenicity issues of HIV p24 antigen by the use of innovative nanostructured lipid carriers as delivery systems: evidences in mice and non-human primates, Npj Vaccines. 3 (2018) 46. doi:10.1038/s41541-018-0086-0.

[16] M. Varache, M. Ciancone, F. Caputo, C. Laffont, M. Escudé, D. Jary, P. Boisseau, I. Texier, F. Navarro, A.-C. Couffin, Development and validation of characterization methods for lipidots® multifunctional platform: A step towards industrial transfer, Adv. Mater. - TechConnect Briefs 2016. 1 (2016) 29–32.

[17] M. Varache, M. Escudé, C. Laffont, E. Rustique, A.-C. Couffin, Development and validation of an HPLC-fluorescence method for the quantification of IR780-oleyl dye in lipid nanoparticles, Int. J. Pharm. 532 (2017) 779–789. doi:10.1016/j.ijpharm.2017.06.019.

[18] Liposome Drug Products: Chemistry, Manufacturing, and Controls; Human Pharmacokinetics and Bioavailability; and Labeling Documentation, (2018) 18.

[19] Reflection paper on the data requirements for intravenous liposomal products developed with reference to an innovator liposomal product, EMA/CHMP/806058/2009/Rev. 02., (2013).

[20] Z. Zhong, Q. Ji, J.A. Zhang, Analysis of cationic liposomes by reversed-phase HPLC with evaporative light-scattering detection, J. Pharm. Biomed. Anal. 51 (2010) 947–951. doi:10.1016/j.jpba.2009.10.001.

[21] M. Oswald, M. Platscher, S. Geissler, A. Goepferich, HPLC analysis as a tool for assessing targeted liposome composition, Int. J. Pharm. 497 (2016) 293–300. doi:10.1016/j.ijpharm.2015.11.014.

[22] D. Jeschek, G. Lhota, J. Wallner, K. Vorauer-Uhl, A versatile, quantitative analytical method for pharmaceutical relevant lipids in drug delivery systems, J. Pharm. Biomed. Anal. 119 (2016) 37–44. doi:10.1016/j.jpba.2015.11.020.

[23] C.B. Roces, E. Kastner, P. Stone, D. Lowry, Y. Perrie, Rapid Quantification and Validation of Lipid Concentrations within Liposomes, Pharmaceutics. 8 (2016). doi:10.3390/pharmaceutics8030029.

[24] S.C. Cunha, M.B.P.P. Oliveira, Discrimination of vegetable oils by triacylglycerols evaluation of profile using HPLC/ELSD, Food Chem. 95 (2006) 518–524. doi:10.1016/j.foodchem.2005.03.029.

[25] N.K. Andrikopoulos, Chromatographic and Spectroscopic Methods in the Analysis of Triacylglycerol Species and Regiospecific Isomers of Oils and Fats, Crit. Rev. Food Sci. Nutr. 42 (2002) 473–505. doi:10.1080/20024091054229.

[26] J.-M. Rabanel, P. Hildgen, X. Banquy, Assessment of PEG on polymeric particles surface, a key step in drug carrier translation, J. Controlled Release. 185 (2014) 71–87. doi:10.1016/j.jconrel.2014.04.017.

[27] T.-L. Cheng, K.-H. Chuang, B.-M. Chen, S.R. Roffler, Analytical Measurement of PEGylated Molecules, Bioconjug. Chem. 23 (2012) 881–899. doi:10.1021/bc200478w.

[28] H. Kim, H.K. Min, G. Kong, M.H. Moon, Quantitative analysis of phosphatidylcholines and phosphatidylethanolamines in urine of patients with breast cancer by nanoflow liquid

chromatography/tandem mass spectrometry, Anal. Bioanal. Chem. 393 (2009) 1649–1656. doi:10.1007/s00216-009-2621-3.

[29] T. Houjou, K. Yamatani, M. Imagawa, T. Shimizu, R. Taguchi, A shotgun tandem mass spectrometric analysis of phospholipids with normal-phase and/or reverse-phase liquid chromatography/electrospray ionization mass spectrometry, Rapid Commun. Mass Spectrom. 19 (2005) 654–666. doi:10.1002/rcm.1836.

[30] V. Verardo, A.M. Gómez-Caravaca, C. Montealegre, A. Segura-Carretero, M.F. Caboni, A. Fernández-Gutiérrez, A. Bendini, Optimization of a solid phase extraction method and hydrophilic interaction liquid chromatography coupled to mass spectrometry for the determination of phospholipids in virgin olive oil, Food Res. Int. 54 (2013) 2083–2090. doi:10.1016/j.foodres.2013.08.026.

[31] M. Schwalbe-Herrmann, J. Willmann, D. Leibfritz, Separation of phospholipid classes by hydrophilic interaction chromatography detected by electrospray ionization mass spectrometry, J. Chromatogr. A. 1217 (2010) 5179–5183. doi:10.1016/j.chroma.2010.05.014.

[32] L. Nováková, L. Matysová, P. Solich, Advantages of application of UPLC in pharmaceutical analysis, Talanta. 68 (2006) 908–918. doi:10.1016/j.talanta.2005.06.035.

[33] D.G. McLaren, P.L. Miller, M.E. Lassman, J.M. Castro-Perez, B.K. Hubbard, T.P. Roddy, An ultraperformance liquid chromatography method for the normal-phase separation of lipids, Anal. Biochem. 414 (2011) 266–272. doi:10.1016/j.ab.2011.03.009.

[34] J.M. Castro-Perez, J. Kamphorst, J. DeGroot, F. Lafeber, J. Goshawk, K. Yu, J.P. Shockcor, R.J. Vreeken, T. Hankemeier, Comprehensive LC–MSE Lipidomic Analysis using a Shotgun Approach and Its Application to Biomarker Detection and Identification in Osteoarthritis Patients, J. Proteome Res. 9 (2010) 2377–2389. doi:10.1021/pr901094j.

[35] M. Kumar, G. Sharma, D. Singla, S. Singh, S. Sahwney, A.S. Chauhan, G. Singh, I.P. Kaur, Development of a validated UPLC method for simultaneous estimation of both free and entrapped (in solid lipid nanoparticles) all-trans retinoic acid and cholecalciferol (vitamin D3) and its pharmacokinetic applicability in rats, J. Pharm. Biomed. Anal. 91 (2014) 73–80. doi:10.1016/j.jpba.2013.12.011.

[36] K.L. Ross, S.L. Hansen, T. Tu, Reversed-phase analysis of triacylglycerols by ultra performance liquid chromatography-evaporative light scattering detection (UPLC-ELSD), Lipid Technol. 23 (2011) 14–16. doi:10.1002/lite.201100083.

[37] J.M. Charlesworth, Evaporative analyzer as a mass detector for liquid chromatography, Anal. Chem. 50 (1978) 1414–1420. doi:10.1021/ac50033a011.

[38] L.M. Nair, J.O. Werling, Aerosol based detectors for the investigation of phospholipid hydrolysis in a pharmaceutical suspension formulation, J. Pharm. Biomed. Anal. 49 (2009) 95–99. doi:10.1016/j.jpba.2008.10.027.

[39] K. Zhang, K.L. Kurita, C. Venkatramani, D. Russell, Seeking universal detectors for analytical characterizations, J. Pharm. Biomed. Anal. 162 (2019) 192–204. doi:10.1016/j.jpba.2018.09.029.

[40] A.M. Descalzo, E.M. Insani, N.A. Pensel, Light-scattering detection of phospholipids resolved by HPLC, Lipids. 38 (2003) 999–1003.

[41] A.E. Mengesha, P.M. Bummer, Simple Chromatographic Method for Simultaneous Analyses of Phosphatidylcholine, Lysophosphatidylcholine, and Free Fatty Acids, AAPS

PharmSciTech. 11 (2010) 1084–1091. doi:10.1208/s12249-010-9470-4.

[42] R. Rombaut, K. Dewettinck, J. Van Camp, Phospho- and sphingolipid content of selected dairy products as determined by HPLC coupled to an evaporative light scattering detector (HPLC–ELSD), J. Food Compos. Anal. 20 (2007) 308–312. doi:10.1016/j.jfca.2006.01.010.

[43] P. Donato, F. Cacciola, F. Cichello, M. Russo, P. Dugo, L. Mondello, Determination of phospholipids in milk samples by means of hydrophilic interaction liquid chromatography coupled to evaporative light scattering and mass spectrometry detection, J. Chromatogr. A. 1218 (2011) 6476–6482. doi:10.1016/j.chroma.2011.07.036.

[44] K.-P. Yan, H.-L. Zhu, N. Dan, C. Chen, An Improved Method for the Separation and Quantification of Major Phospholipid Classes by LC-ELSD, Chromatographia. 72 (2010) 815–819. doi:10.1365/s10337-010-1759-7.

[45] H. Shibata, C. Yomota, H. Okuda, Simultaneous Determination of Polyethylene Glycol-Conjugated Liposome Components by Using Reversed-Phase High-Performance Liquid Chromatography with UV and Evaporative Light Scattering Detection, AAPS PharmSciTech. 14 (2013) 811–817. doi:10.1208/s12249-013-9967-8.

[46] V. Zabaleta, M.A. Campanero, J.M. Irache, An HPLC with evaporative light scattering detection method for the quantification of PEGs and Gantrez in PEGylated nanoparticles, J. Pharm. Biomed. Anal. 44 (2007) 1072–1078. doi:10.1016/j.jpba.2007.05.006.

[47] B.N. Barman, D.H. Champion, S.L. Sjoberg, Identification and quantification of polyethylene glycol types in polyethylene glycol methyl ether and polyethylene glycol vinyl ether, J. Chromatogr. A. 1216 (2009) 6816–6823. doi:10.1016/j.chroma.2009.08.024.

[48] J.H. Arndt, T. Macko, R. Brüll, Application of the evaporative light scattering detector to analytical problems in polymer science, J. Chromatogr. A. 1310 (2013) 1–14. doi:10.1016/j.chroma.2013.08.041.

[49] W.-J. Lee, N.-W. Su, M.-H. Lee, J.-T. Lin, Assessment of authenticity of sesame oil by modified Villavecchia Test and HPLC-ELSD analysis of triacylglycerol profile, Food Res. Int. 53 (2013) 195–202. doi:10.1016/j.foodres.2013.04.008.

[50] E. Lesellier, A. Latos, A.L. de Oliveira, Ultra high efficiency/low pressure supercritical fluid chromatography with superficially porous particles for triglyceride separation, J. Chromatogr. A. 1327 (2014) 141–148. doi:10.1016/j.chroma.2013.12.046.

[51] W.E. Neff, G.R. List, W.C. Byrdwell, Quantitative Composition of High Palmitic and Stearic Acid Soybean Oil Triacylglycerols by Reversed Phase High Performance Liquid Chromatography: Utilization of Evaporative Light Scattering and Flame Ionization Detectors, J. Liq. Chromatogr. Relat. Technol. 22 (1999) 1649–1662. doi:10.1081/JLC-100101758.

[52] F. Donot, G. Cazals, Z. Gunata, D. Egron, J. Malinge, C. Strub, A. Fontana, S. Schorr-Galindo, Analysis of neutral lipids from microalgae by HPLC-ELSD and APCI-MS/MS, J. Chromatogr. B Analyt. Technol. Biomed. Life. Sci. 942–943 (2013) 98–106. doi:10.1016/j.jchromb.2013.10.016.

[53] K. Vorauer-Uhl, D. Jeschek, G. Lhota, A. Wagner, S. Strobach, H. Katinger, Simultaneous Quantification of Complex Phospholipid Compositions Containing Monophosphoryl Lipid-A by RP-HPLC, J. Liq. Chromatogr. Relat. Technol. 32 (2009) 2203–2215. doi:10.1080/10826070903163180.

[54] M.M. Alsaadi, K. Christine Carter, A.B. Mullen, High performance liquid chromatography with evaporative light scattering detection for the characterisation of a vesicular delivery system during stability studies, J. Chromatogr. A. 1320 (2013) 80–85. doi:10.1016/j.chroma.2013.10.054.

[55] N.C. Megoulas, M.A. Koupparis, Twenty Years of Evaporative Light Scattering Detection, Crit. Rev. Anal. Chem. 35 (2005) 301–316. doi:10.1080/10408340500431306.

[56] R. Lucena, S. Cárdenas, M. Valcárcel, Evaporative light scattering detection: trends in its analytical uses, Anal. Bioanal. Chem. 388 (2007) 1663–1672. doi:10.1007/s00216-007-1344-6.

[57] R.A. Moreau, Lipid analysis via HPLC with a charged aerosol detector, Lipid Technol. 21 (2009) 191–194. doi:10.1002/lite.200900048.

[58] A. Avalli, G. Contarini, Determination of phospholipids in dairy products by SPE/HPLC/ELSD, J. Chromatogr. A. 1071 (2005) 185–190. doi:10.1016/j.chroma.2005.01.072.

[59] J. Gravier, F.P. Navarro, T. Delmas, F. Mittler, A.-C. Couffin, F. Vinet, I. Texier, Lipidots: competitive organic alternative to quantum dots for in vivo fluorescence imaging, J. Biomed. Opt. 16 (2011) 096013. doi:10.1117/1.3625405.

[60] A. Jacquart, M. Kéramidas, J. Vollaire, R. Boisgard, G. Pottier, E. Rustique, F. Mittler, F.P. Navarro, J. Boutet, J.-L. Coll, I. Texier, LipImage™ 815: Novel dye-loaded lipid nanoparticles for long-term and sensitive in vivo near-infrared fluorescence imaging, J. Biomed. Opt. 18 (2013). doi:10.1117/1.JBO.18.10.101311.

[61] M. Buchgraber, F. Ulberth, H. Emons, E. Anklam, Triacylglycerol profiling by using chromatographic techniques, Eur. J. Lipid Sci. Technol. 106 (2004) 621–648. doi:10.1002/ejlt.200400986.

[62] A. Ruiz-Rodriguez, G. Reglero, E. Ibañez, Recent trends in the advanced analysis of bioactive fatty acids, J. Pharm. Biomed. Anal. 51 (2010) 305–326. doi:10.1016/j.jpba.2009.05.012.

[63] S. Indelicato, D. Bongiorno, R. Pitonzo, V. Di Stefano, V. Calabrese, S. Indelicato, G. Avellone, Triacylglycerols in edible oils: Determination, characterization, quantitation, chemometric approach and evaluation of adulterations, J. Chromatogr. A. 1515 (2017) 1–16. doi:10.1016/j.chroma.2017.08.002.

[64] M.J. Wojtusik, P.R. Brown, J.G. Turcotte, Separation and detection of triacylglycerols by high-performance liquid chromatography, Chem. Rev. 89 (1989) 397–406. doi:10.1021/cr00092a009.

[65] A. Zeb, M. Murkovic, Analysis of triacylglycerols in refined edible oils by isocratic HPLC-ESI-MS, Eur. J. Lipid Sci. Technol. 112 (2010) 844–851. doi:10.1002/ejlt.201000064.

[66] W.E. Neff, W.C. Byrdwell, Soybean oil triacylglycerol analysis by reversed-phase high-performance liquid chromatography coupled with atmospheric pressure chemical ionization mass spectrometry, J. Am. Oil Chem. Soc. 72 (1995) 1185–1191. doi:10.1007/BF02540986.

[67] R. Rombaut, N.D. Clercq, I. Foubert, K. Dewettinck, Triacylglycerol Analysis of Fats and Oils by Evaporative Light Scattering Detection, J. Am. Oil Chem. Soc. 86 (2009) 19–25. doi:10.1007/s11746-008-1316-9.

[68] R.D. Plattner, G.F. Spencer, R. Kleiman, Triglyceride separation by reverse phase high performance liquid chromatography, J. Am. Oil Chem. Soc. 54 (1977) 511–515. doi:10.1007/BF02909070.

[69] Avanti Polar Lipids, Avanti Polar Lipids. (n.d.). https://avantilipids.com/ (accessed September 9, 2018).

[70] Y.H. Lee, E.S. Jeong, H.E. Cho, D.-C. Moon, Separation and determination of polyethylene glycol fatty acid esters in cosmetics by a reversed-phase HPLC/ELSD, Talanta. 74 (2008) 1615–1620. doi:10.1016/j.talanta.2007.10.020.

[71] C. Zhu, A. Dane, G. Spijksma, M. Wang, J. van der Greef, G. Luo, T. Hankemeier, R.J. Vreeken, An efficient hydrophilic interaction liquid chromatography separation of 7 phospholipid classes based on a diol column, J. Chromatogr. A. 1220 (2012) 26–34. doi:10.1016/j.chroma.2011.11.034.

[72] A.J. Alpert, Hydrophilic-interaction chromatography for the separation of peptides, nucleic acids and other polar compounds, J. Chromatogr. 499 (1990) 177–196.

[73] S. Granafei, P. Azzone, V.A. Spinelli, I. Losito, F. Palmisano, T.R.I. Cataldi, Hydrophilic interaction and reversed phase mixed-mode liquid chromatography coupled to high resolution tandem mass spectrometry for polar lipids analysis, J. Chromatogr. A. 1477 (2016) 47–55. doi:10.1016/j.chroma.2016.11.048.

[74] G. Marrubini, P. Appelblad, M. Maietta, A. Papetti, Hydrophilic interaction chromatography in food matrices analysis: An updated review, Food Chem. 257 (2018) 53–66. doi:10.1016/j.foodchem.2018.03.008.

[75] L. Nováková, L. Havlíková, H. Vlčková, Hydrophilic interaction chromatography of polar and ionizable compounds by UHPLC, TrAC Trends Anal. Chem. 63 (2014) 55–64. doi:10.1016/j.trac.2014.08.004.

[76] D.V. McCalley, Understanding and manipulating the separation in hydrophilic interaction liquid chromatography, J. Chromatogr. A. 1523 (2017) 49–71. doi:10.1016/j.chroma.2017.06.026.

[77] A. Guillot, A.-C. Couffin, X. Sejean, F. Navarro, M. Limberger, C.-M. Lehr, Solid Phase Extraction as an Innovative Separation Method for Measuring Free and Entrapped Drug in Lipid Nanoparticles, Pharm. Res. (2015) 1–11. doi:10.1007/s11095-015-1761-8.

[78] K. Mojsiewicz-Pieńkowska, On the Issue of Characteristic Evaporative Light Scattering Detector Response, Crit. Rev. Anal. Chem. 39 (2009) 89–94. doi:10.1080/15389580802570218.

[79] B.T. Mathews, P.D. Higginson, R. Lyons, J.C. Mitchell, N.W. Sach, M.J. Snowden, M.R. Taylor, A.G. Wright, Improving Quantitative Measurements for the Evaporative Light Scattering Detector, Chromatographia. 60 (2004) 625–633. doi:10.1365/s10337-004-0441-3.

[80] C. Orellana-Coca, D. Adlercreutz, M.M. Andersson, B. Mattiasson, R. Hatti-Kaul, Analysis of fatty acid epoxidation by high performance liquid chromatography coupled with evaporative light scattering detection and mass spectrometry, Chem. Phys. Lipids. 135 (2005) 189–199. doi:10.1016/j.chemphyslip.2005.02.014.

[81] W. Li, J.F. Fitzloff, Determination of 24(R)-pseudoginsenoside F11 in North American ginseng using high performance liquid chromatography with evaporative light scattering detection, J. Pharm. Biomed. Anal. 25 (2001) 257–265. doi:10.1016/S0731-7085(00)00494-

5.

[82] G.A. Picchioni, A.E. Watada, B.D. Whitaker, Quantitative high-performance liquid chromatography analysis of plant phospholipids and glycolipids using light-scattering detection, Lipids. 31 (1996) 217–221.

[83] ICH guideline Q2(R1) : Validation of Analytical Procedures : Text and Methodology, (2005).

[84] H.J. Motulsky, L.A. Ransnas, Fitting curves to data using nonlinear regression: a practical and nonmathematical review., FASEB J. 1 (1987) 365–374. doi:10.1096/fasebj.1.5.3315805.

[85] R.G. Ramos, D. Libong, M. Rakotomanga, K. Gaudin, P.M. Loiseau, P. Chaminade, Comparison between charged aerosol detection and light scattering detection for the analysis of Leishmania membrane phospholipids, J. Chromatogr. A. 1209 (2008) 88–94. doi:10.1016/j.chroma.2008.07.080.

[86] T. Delmas, H. Piraux, A.-C. Couffin, I. Texier, F. Vinet, P. Poulin, M.E. Cates, J. Bibette, How To Prepare and Stabilize Very Small Nanoemulsions, Langmuir. 27 (2011) 1683–1692. doi:10.1021/la104221q.

[87] J.A. Zhang, J. Pawelchak, Effect of pH, ionic strength and oxygen burden on the chemical stability of EPC/cholesterol liposomes under accelerated conditions. Part 1: Lipid hydrolysis, Eur. J. Pharm. Biopharm. Off. J. Arbeitsgemeinschaft Pharm. Verfahrenstechnik EV. 50 (2000) 357–364.

[88] L. Rabinovich-Guilatt, C. Dubernet, K. Gaudin, G. Lambert, P. Couvreur, P. Chaminade, Phospholipid hydrolysis in a pharmaceutical emulsion assessed by physicochemical parameters and a new analytical method, Eur. J. Pharm. Biopharm. 61 (2005) 69–76. doi:10.1016/j.ejpb.2005.03.001.

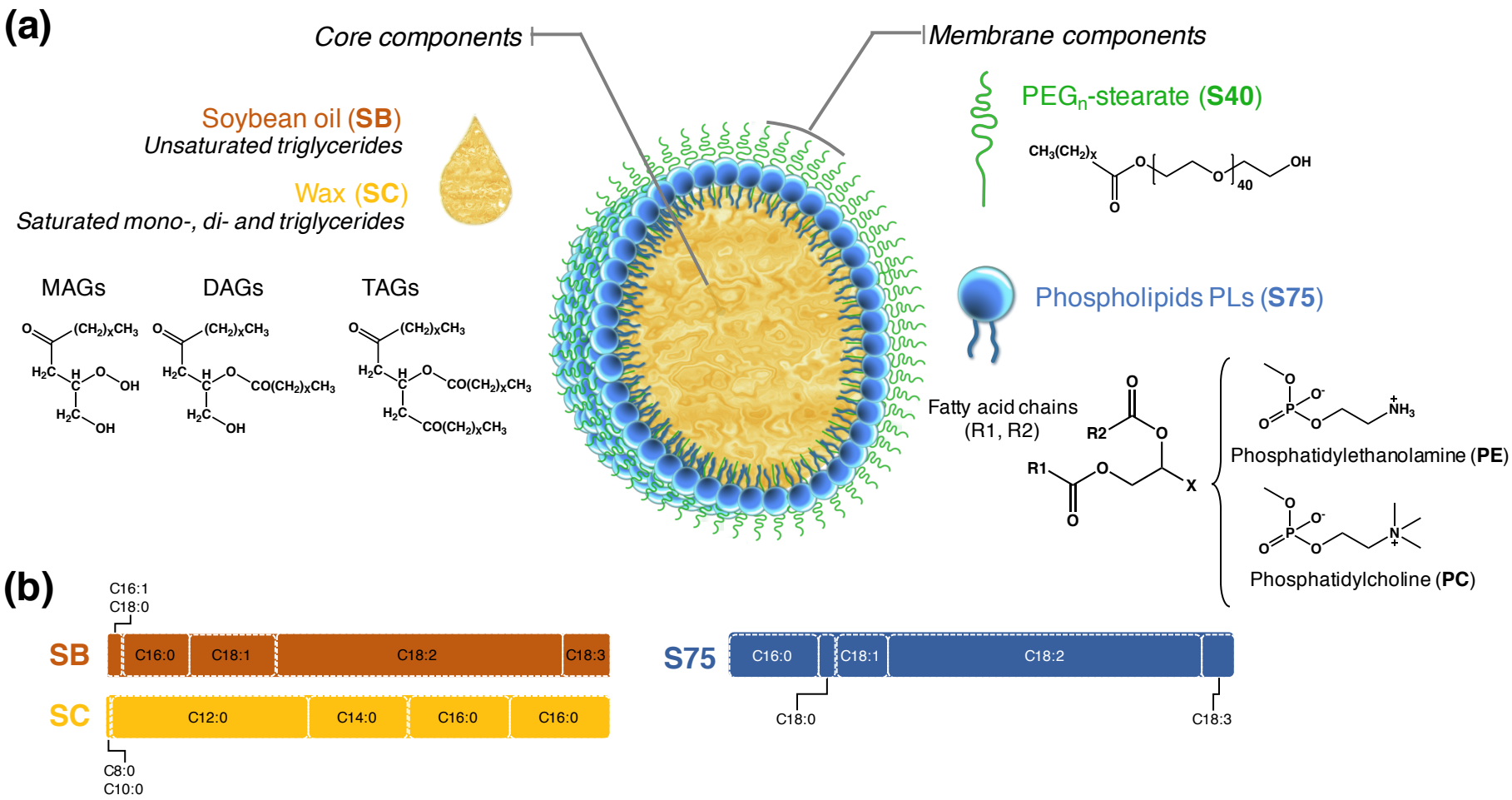

Figure 1: (a) Structure and composition of the lipid excipients incorporated in the preparation of lipid nanoparticles, and (b) Fatty acid composition (average) of SB, SC and S75 according to the manufacturer.

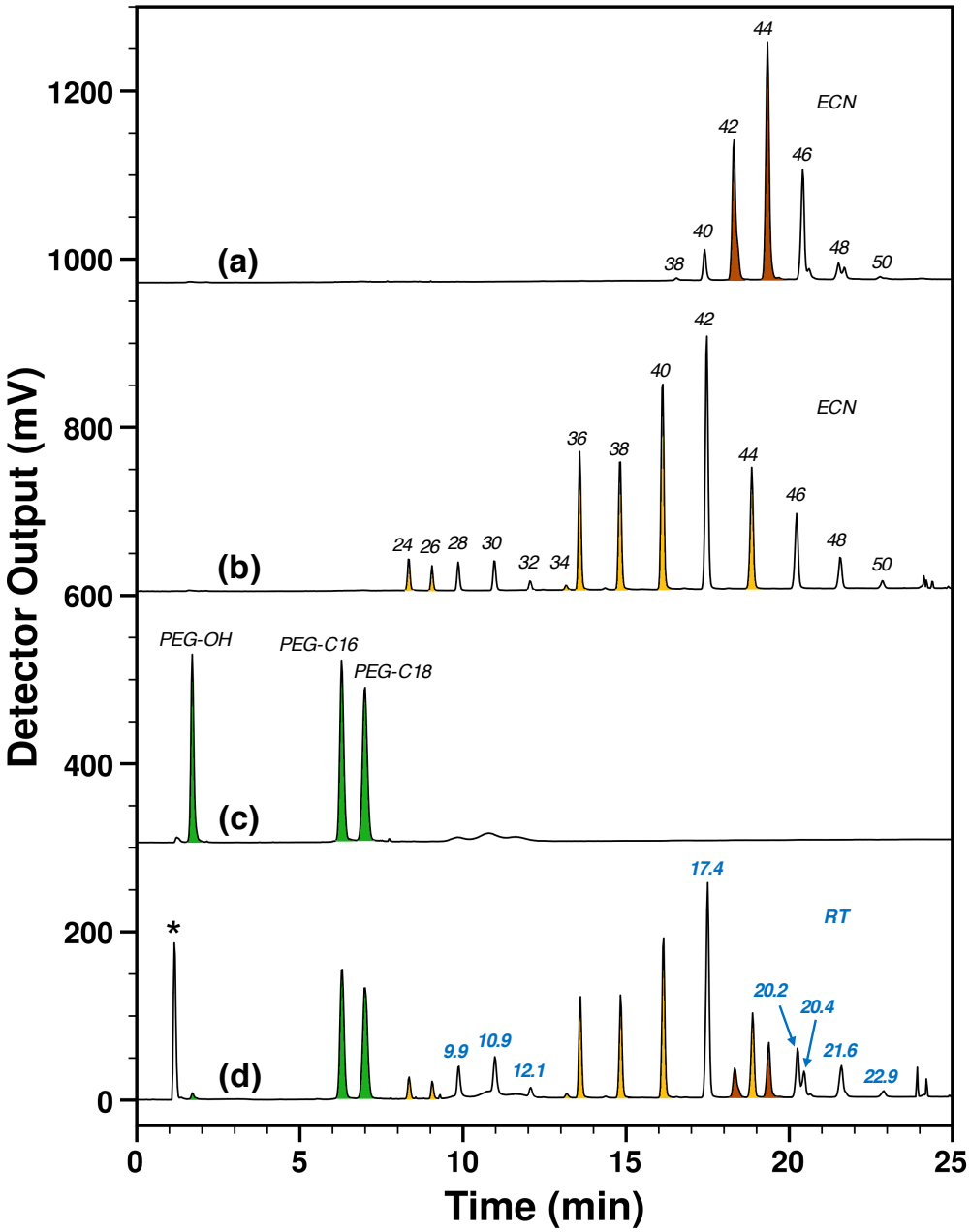

Figure 2: RP-UPLC-ELSD chromatograms using QMC18 of (a) SB at 190 μg/mL, (b) SC at 500 μg/mL, (c) S40 at 569 μg/mL, as crude excipients and (d) a nanoparticle suspension after sample preparation (1100 μg/mL: theoretical concentration of total lipid excipients). Samples were prepared in a mixture of $CHCl_3$ and MeOH (2:1, v/v). The first peak labelled with a star (*) symbol was identified as PBS. For SB and SC, each peak was labelled with the ECN. Peak overlap between SC and SB was identified by uncolored peaks labelled with retention times in green. Peaks of each component used to determine the area under the curve have been highlighted in green, yellow and brown for PEG components, SC and SB, respectively.

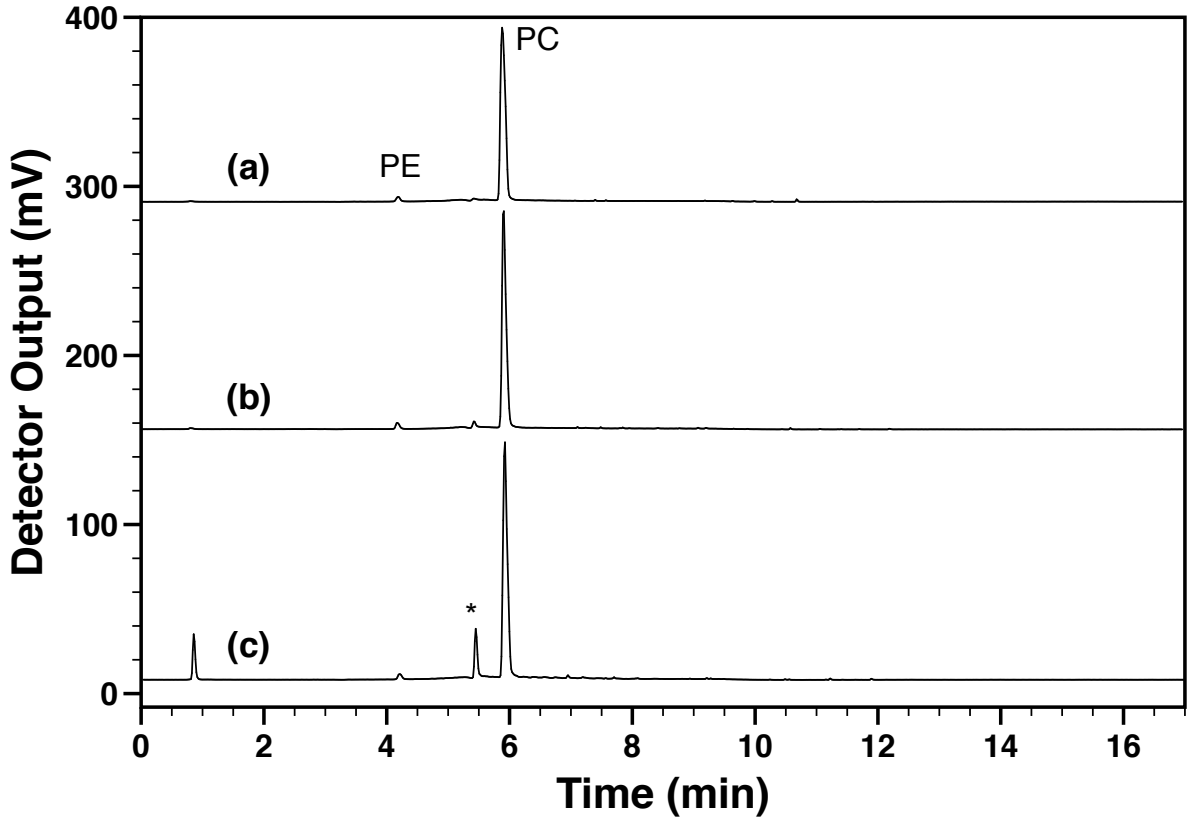

Figure 3: HILIC-UPLC-ELSD chromatograms using QMHILIC for (a) standards of Soy PC and Soy PE at 152 and 22 μg/mL, respectively, (b) Lipoid S75 as crude excipient at 217 μg/mL and (c) a nanoparticle suspension after sample preparation including SPE separation. Peak labelled with a star (*) symbol was identified as PBS.

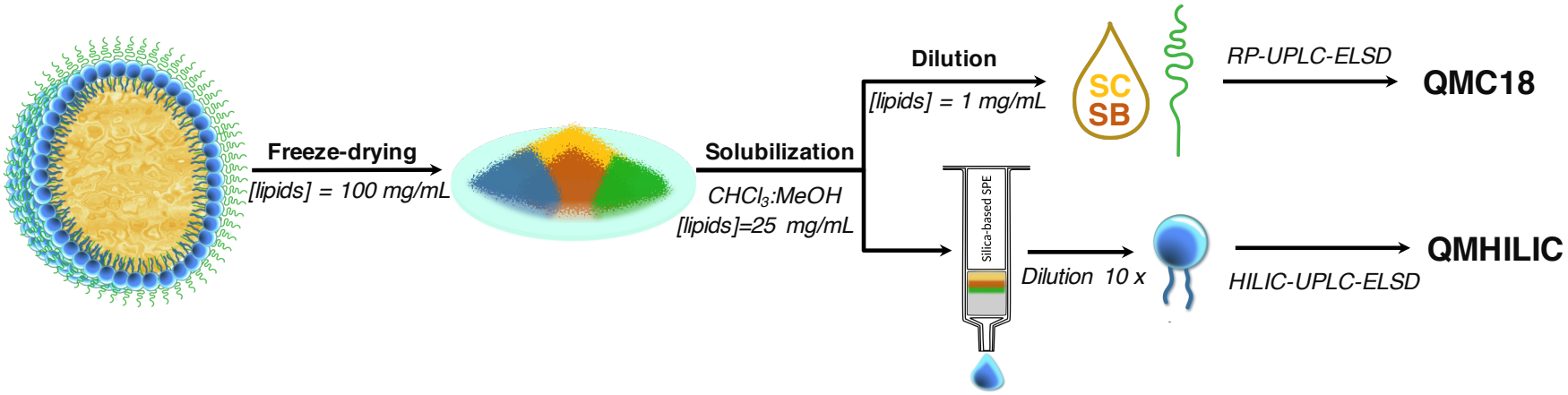

Figure 4: Sample preparation process.

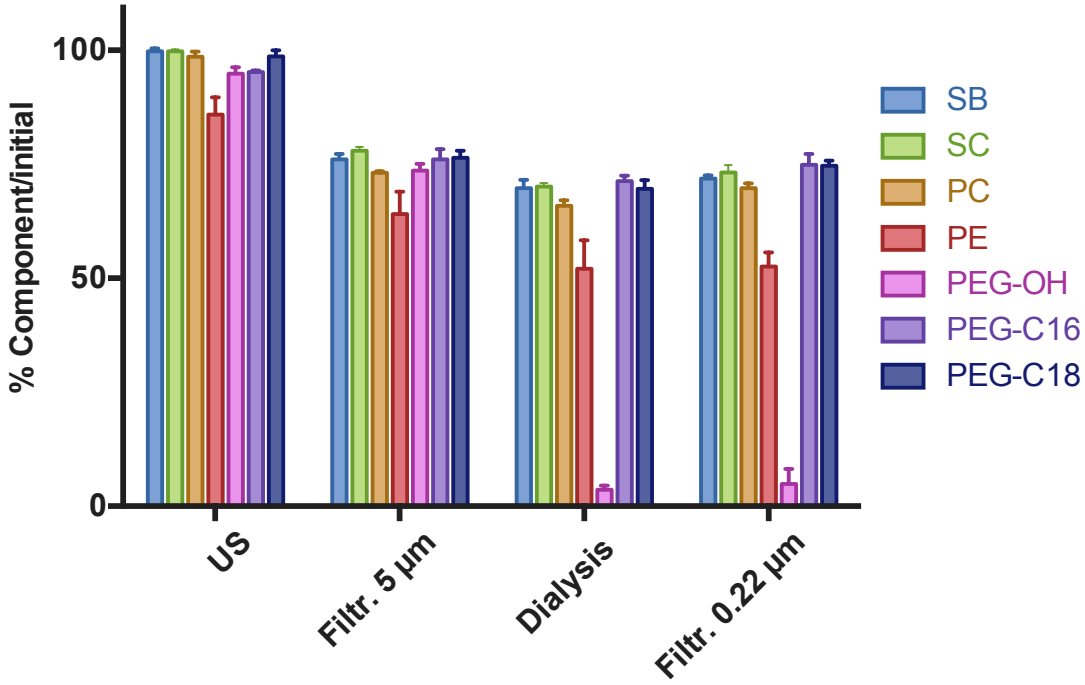

Figure 5: Evolution of lipids content along the formulation process. Each bar represents the remaining quantity of component after each step, compared to the quantity initially introduced in the formulation process (before sonication).

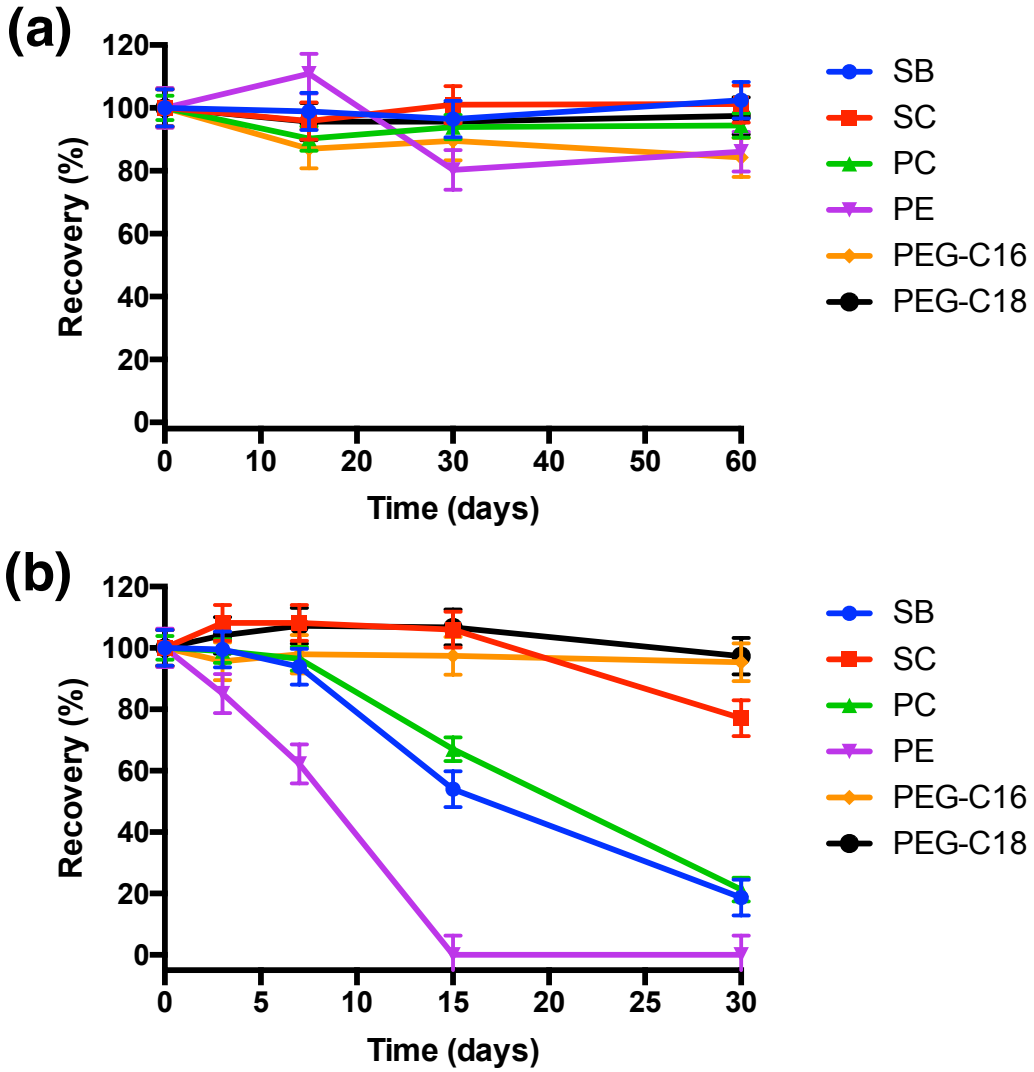

Figure 6: Evolution of lipid contents extracted from 50 nm nanoparticle suspensions stored at (a) 4°C or (b) 60°C.

Table 1: Gradient elution program used for the analysis of lipids belonging to Soybean (SB) oil, Suppocire (SC) and Myrj S40 (S40) using 100% water (A), 100% methanol (B) and a mixture of isopropanol and acetonitrile in a volume ratio of 75:25 (v/v) (C). This method is referred as "QMC18" in the manuscript.

Time (min)	Flow rate (mL/min)	A (%)	B (%)	C (%)	Analyte
0.0	0.25	30	70	0	
3.0	0.30	10	90	0	**S40**
7.0	0.30	0	100	0	
7.0	0.30	0	100	0	
22.0	0.30	0	35	65	**SC/SB**
25.0	0.30	0	35	65	
25.1	0.25	30	70	0	**Equilibration**
30.0	0.25	30	70	0	

Table 2: Analytical parameters corresponding to QMC18 and QMHILIC methods.

Method	QMC18	QMHILIC
HPLC setup	• **Column:** CORTECS UPLC C18 (1.6 µm ; 150 x 2.1 mm, 90 Å) • **Guard:** CORTECS UPLC C18 (1.6 µm ; 5 x 2.1 mm, 90 Å) • **Temperature:** 40°C • **Mobile phases:** MQ, MeOH, IPA/ACN • **Flow rate:** 0.25-0.3 mL/min • **Elution mode:** Gradient • **Injection volume:** 5 µL • **Run duration:** 30 min	• **Column:** CORTECS UPLC HILIC (1.6 µm ; 150 x 2.1 mm, 90 Å) • **Guard:** CORTECS UPLC HILIC (1.6 µm ; 5 x 2.1 mm, 90 Å) • **Temperature:** 40°C • **Mobile phases:** ACN, 10 mM ammonium formate (pH=3) • **Flow rate:** 0.5 mL/min • **Elution mode:** Gradient • **Injection volume:** 5 µL • **Run duration:** 17 min
ELSD setup	• **N_2 flow:** 2.0 L/min • **Drift tube:** 45°C • **Gain: 4**	• **N_2 flow:** 2.5 L/min • **Drift tube:** 60°C • **Gain: 2**
Compound	• **SB:** 15 TAGs • **SC:** 15 TAGs and DAGs • **S40:** PEG-OH, PEG-C16 and PEG-C18	• **S75:** PC and PE
Total lipid concentration (analysis)	• 1 mg/mL	• 2.5 mg/mL
Analysis concentration	• **SB:** 113.3 µg/mL • **SC:** 340 µg/mL • **S40:** 460 µg/mL	• **S75:** 216.7 µg/mL
Diluent	• $CHCl_3$:MeOH (2:1, v/v)	• **SPE** elution with MeOH and $CHCl_3$:MeOH:MQ (3:5:2, v/v/v)

Table 3: Second order polynomial equation for calibration, limit of detection (LOD) and quantification (LOQ) for the components. Five concentrations of each compound were analyzed in triplicate. The data were fitted with a quadratic equation $Y = a_0X^2 + a_1X + a_2$, where X represents the concentration in µg/mL, a_0, a_1, and a_2 are constants for the equations and Y is the peak area. Calibration curves for PLs were determined after adding the other crude excipients (SB, SC and S40) and applying the SPE process.

Coumpound	Target[a] conc. (µg/mL)	Calibration range (µg/mL)	Equation	R^2	LOD (µg/mL)	LOQ (µg/mL)
SB	133.3	45.4 - 136.1	$Y = 40.105X^2 + 1146X - 26191$	0.9991	6.2	20.8
SC	340.0	135.8 - 407.9	$Y = 26.187X^2 – 1888X + 292559$	0.9993	8.2	27.4
PEG-OH	100.0	62.0 - 186.1	$Y = 46.325X^2 + 2729.7X - 63935$	0.9999	0.8	2.3
PEG-C16	115.0	62.0 - 186.1	$Y = 46.645X^2 + 3849.9X -139327$	0.9991	ND	ND
PEG-C18	115.0	62.0 - 186.1	$Y = 46.278X^2 + 4219.2X -143828$	0.9999	ND	ND
Soy PE	21.7	8.7 - 26.0	$Y = 10.552X^2 + 439.9X - 12$	0.9977	2.9	8.7
Soy PC	151.6	60.6 - 182.0	$Y = 10.530X^2 + 3099.2X - 80715$	0.9991	4.8	16.0

[a]Concentration at 100% of the components (expected concentration for a nanoparticle suspension following the sample preparation process).

Table 4: Accuracy and precision at three levels (60, 100 and 120%) to bracket the concentrations used in the nanoparticle formulations.

Lipid	Target[a] conc. (%)	Spiked conc. (µg/mL)	Measured conc. (µg/mL)	RSD (%)	RE (%)
SB	60%	68.0	69.2	2.5%	101.8%
	100%	113.3	127.1	1.6%	112.2%
	120%	136.0	144.8	5.3%	106.5%
SC	60%	203.8	205.0	4.9%	100.5%
	100%	339.9	366.4	1.1%	107.8%
	120%	407.9	404.6	4.0%	99.2%
PEG-OH	60%	60.0	57.4	1.8%	97.6%
	100%	100.0	94.1	1.9%	96.0%
	120%	119.9	115.8	1.2%	98.5%
PEG-C16	60%	69.0	61.7	1.2%	89.5%
	100%	115.0	104.9	1.5%	91.2%
	120%	137.8	129.5	0.9%	93.8%
PEG-C18	60%	68.9	57.6	2.1%	83.5%
	100%	115.0	104.3	1.1%	90.7%
	120%	137.8	128.0	1.1%	92.7%
Soy PE	60%	13.0	11.2	3.4%	86.4%
	100%	21.7	21.1	1.4%	97.5%
	120%	26.0	23.8	1.0%	91.7%
Soy PC	60%	91.0	83.6	2.5%	91.8%
	100%	151.6	146.2	0.9%	96.4%
	120%	182.0	180.4	1.3%	99.1%

[a]100%: Theoretical concentration for nanoparticle suspensions after sample preparation (analysis concentration).

Table 5: System repeatability, intra-day and inter-day precision performed using nanoparticle suspensions. Concentrations are expressed in milligrams per mL of a suspension at 100 mg/mL of lipids. Experimental concentrations were calculated by weighing the sample after the freeze-drying process (1 mL of suspension at 100 mg/mL of lipids per sample). The percent recovery (%) was calculated based on theoretical and experimental concentrations.

		System repeatability (n=6)		**Day 1 (n=3)**		**Day 2 (n=3)**		**Day 3 (n=3)**		**Overall (n=9)**		**Overall Recovery**	
Lipid	Theo. conc.	Exp. conc.	RSD (%)	Exp. conc.	RSD (%)	Exp. conc.	RSD (%)	Exp. conc.	RSD (%)	Exp. conc.	RSD (%)	(%)	RSD (%)
SB	11.33	7.99	2.6%	10.86	2.8%	11.57	5.6%	9.77	2.3%	10.62	5.9%	93.7	8.5%
SC	34.00	29.19	1.5%	32.57	3.8%	33.51	3.6%	32.48	7.1%	33.10	5.9%	97.3	1.7%
PEG-OH	9.88	0.30	5.9%	0.40	5.0%	0.31	4.7%	0.31	7.1%	0.35	14.3%	3.5	15.9%
PEG-C16	11.34	9.93	1.0%	9.18	2.5%	10.03	3.7%	10.43	3.6%	9.92	6.2%	87.5	6.4%
PEG-C18	11.57	9.68	1.3%	9.11	2.9%	9.84	3.9%	10.22	3.9%	9.76	5.9%	84.4	5.8%
PE	0.87	0.72	1.0%	0.81	6.0%	0.79	4.2%	0.73	2.5%	0.78	6.3%	89.9	5.5%
PC	6.07	5.22	1.0%	5.75	3.6%	5.58	1.5%	5.59	5.3%	5.64	3.9%	92.9	1.7%

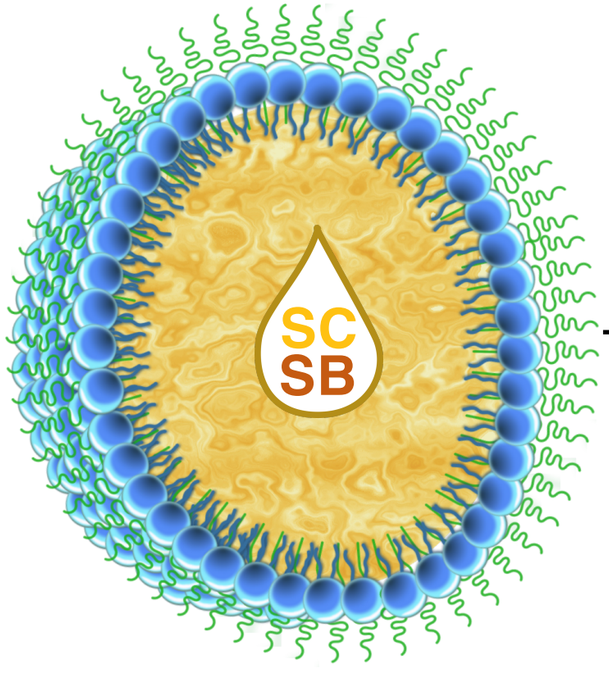

Freeze-drying

Wax (SC)

Soybean oil (**SB**)

PEG_n-stearate (**S40**)

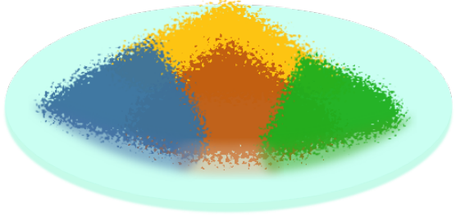

Phospholipids PLs (**S75**)

RP-UPLC-ELSD

QMC18

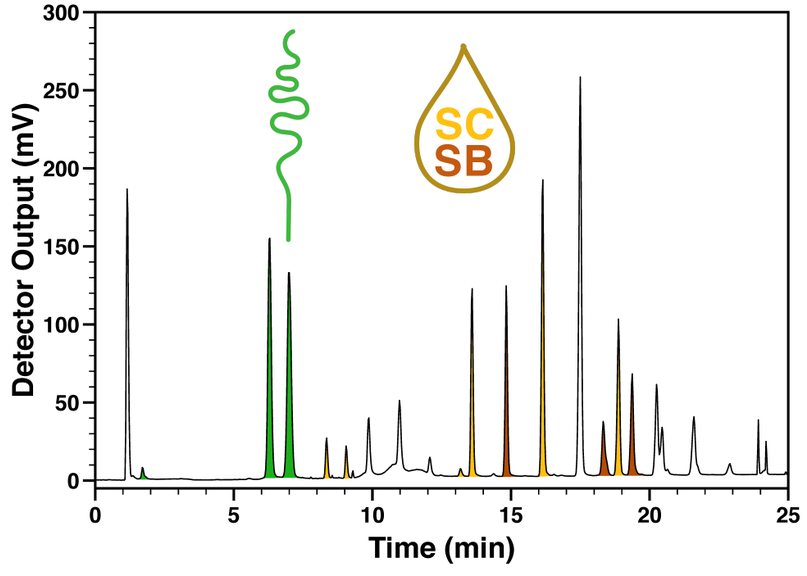

HILIC-UPLC-ELSD

QMHILIC